



## Review

# CT in planning transcatheter aortic valve implantation procedures and risk assessment

A. Yucel-Finn<sup>a</sup>, E. Nicol<sup>b</sup>, J.A. Leipsic<sup>c</sup>, J.R. Weir-McCall<sup>a,d,\*</sup><sup>a</sup>Royal Papworth Hospital, Cambridge, UK<sup>b</sup>Royal Brompton Hospital, London, UK<sup>c</sup>St Paul's Hospital, Vancouver, British Columbia, Canada<sup>d</sup>University of Cambridge School of Clinical Medicine, Cambridge, UK

For surgical aortic valve replacement, the Society of Thoracic Surgeons score (STSS) is the reference standard for the prediction of operative risk. In transcatheter aortic valve implantation (TAVI) though, where the procedure itself is minimally invasive, the traditional risk assessment is supplemented by CTA. Through a consistent approach to the acquisition of high-quality images and the standardised reporting of annular measurements and adverse root and vascular features, patients at risk of complications can be identified. In turn, this may allow for a personalised procedural approach and treatment strategies devised to potentially reduce or mitigate this risk. This article provides a systematic and standardised approach to pre-procedural work-up with computed tomography angiography (CTA) and explores the current state of evidence and future areas of development in this rapidly developing field.

© 2019 The Royal College of Radiologists. Published by Elsevier Ltd. All rights reserved.

## Introduction

Transcatheter aortic valve implantation (TAVI, also known as Transcatheter aortic valve replacement [TAVR]) was first performed in 2002.<sup>1</sup> Since this time, the use of TAVI has expanded in volume as its evidence across an increasing range of patient cohorts has grown. Initially, the TAVI procedure was reserved for those deemed inoperable and surgically high risk.<sup>2</sup> Multiple randomised control trials, including the recent PARTNER 3 and Evolut trials, have subsequently proven the efficacy of TAVI for intermediate and low-risk patients compared with surgically implanted

valve replacements.<sup>3,4</sup> In parallel with these trials the evidence supporting the role of computed tomography (CT) angiography (CTA) in procedural planning has grown and is generally favourable (Fig 1).

Imaging has a key role to play in the evaluation of patients considered for TAVI.<sup>5,6</sup> The advent of electrocardiogram (ECG)-gated CT acquisition has enabled motion-free images of the aortic root to be acquired with exquisite anatomical detail. The majority of the information required for TAVI transcatheter heart valve (THV) selection and implantation can be gleaned from the CT TAVI dataset: annular and root dimensions and geometry can be measured; high-risk features for adverse events, such as coronary occlusion, annular injury, and post-TAVI conduction abnormalities can be detected and the lowest risk transcatheter access route determined. Valve-in-valve TAVI similarly benefits from pre-procedural CTA, although requires a completely different framework of assessment.

\* Guarantor and correspondent: J. R. Weir-McCall, University of Cambridge School of Clinical Medicine, Box 219, Level 5, Biomedical Campus, Cambridge, CB2 0QQ, UK. Tel: 01223 638000.

E-mail address: [jw2079@cam.ac.uk](mailto:jw2079@cam.ac.uk) (J.R. Weir-McCall).

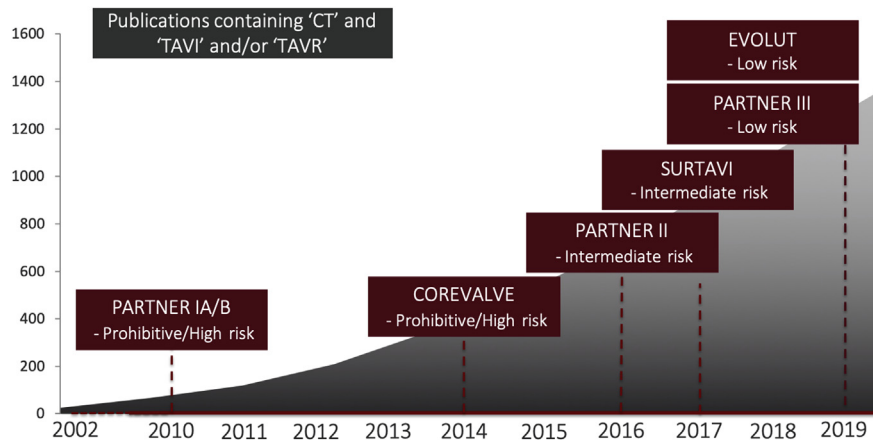


**Figure 1** The growth of literature exploring the use of CTA in TAVI work-up as the evidence base supporting its use has grown.

This article provides an overview of the key facets of CT for TAVI, from acquisition of the TAVI dataset, interpretation and key findings, and a glimpse into future developments likely to impact on clinical practice.

## The CT TAVI dataset

An ECG-gated dataset allows for motion-free assessment of the aortic root. In the formative years of TAVI, CTA was often limited to the aortic arch to mid-femoral arteries. More recently, however, as the number of access sites has increased, the TAVI dataset now often is extended to include the subclavians to mid-femoral arteries. In centres that use the carotid artery as an access route, inclusion of the carotids and circle of Willis extends this scan range further, and ensuring adequate cerebral vascular supply is a critical determinant of patient suitability for this approach. Ideally, scans should be undertaken in a combined approach with only one dose of contrast medium given. Additionally, a pre-contrast calcium score dataset and a separate assessment of the coronary arteries may also be added. An overview of guidance to acquire suitable CT images necessary for TAVI planning is provided below.

## Patient preparation

As for any contrast-enhanced study, intravenous access is required, and should be through a minimum 20-G cannula. A dual head injector is required for correct contrast medium timing and is necessary to achieve overlap between ECG-synchronisation and contrast delivery. Chronic kidney disease is relatively prevalent in those referred for TAVI; however, special precautions are no longer recommended for patients with estimated glomerular filtration rate (eGFR)  $>45$  ml/min/1.73m<sup>2</sup>. Additionally, the risk for those in the 30–45 ml/min/1.73m<sup>2</sup> bracket is considered low and peri-procedural hydration is no longer indicated.<sup>7</sup> In severe renal impairment, cautious pre-scan intravenous hydration with 0.9% intravenous saline is suggested, but local agreed protocols should be followed as for any contrast-enhanced CT

study.<sup>7</sup> Unenhanced acquisitions may allow limited visualisation that may remain useful to the interventionist.

## Acquisition

During protocolling for CT TAVI, the addition of an aortic valve calcium score should be considered. Although most aortic stenosis is graded accurately using echocardiography, in around 25% of cases there remains uncertainty as to the true severity of aortic stenosis, and calcium scoring can assist in determining this.<sup>8</sup> The aortic valve calcium score has been shown to provide excellent discrimination for severe aortic stenosis with gender-specific thresholds.<sup>8–10</sup> For men, a score of  $>2,062$  AU, and for women  $>1,377$  AU, are strongly indicative of severe aortic stenosis. This is performed as for coronary artery calcium Agatston scoring, prior to the CTA TAVI contrast acquisition.

The challenge of a CTA TAVI scan is often how to combine an ECG-gated dataset of the aortic root structures with a vascular CT angiogram from skull (or subclavians if carotid information is not required) to upper-thigh. At present, there are three commonly used strategies (or variations thereof): (1) initial ECG-gated scan of the aortic root followed by a standard vascular CT angiogram from skull base to upper-thigh. This approach images the aortic root and cardiac structures twice. This, however, decreases the dose, compared to a fully gated scan, as it limits the ECG-gated scan range, which is the most dose-intensive. (2) Single acquisition with ECG-gating from the skull to thorax, followed by non-ECG-gated scan from the abdomen to upper thigh. Given the extra time taken for imaging of the thorax, this method is more susceptible to breathing artefact. (3) High-pitch single-phase ECG-gated acquisition of the vasculature and cardiac structures in a single scanning volume, with this timed to acquire the heart at mid systole.

Intra-arterial opacification  $>250$  HU, at the level of the ascending aorta, is recommended.<sup>11</sup> Contrast medium volumes of 50–100 ml, at rate of 4–6 ml, are typically required, with the precise rate and volume dependent on the hardware in use, patient size, and scanning technique in use. Lower doses of contrast medium administered at lower

rates of 3 ml/s coupled with lower tube voltage can be achieved with high image quality irrespective of the use of 64-section,<sup>12</sup> wide-bore,<sup>13–15</sup> or dual-source<sup>16–18</sup> scanner technology, and should be used in those with chronic kidney disease. Future developments in dual energy and spectral imaging allowing for mono-energetic reconstruction techniques may allow for lower volumes of contrast medium in future.<sup>19</sup>

### Radiation dose considerations

The necessity of an ECG-gated aortic root dataset in addition to a near whole-body CT angiogram increases the dose compared with a standard CT angiogram acquisition. Nevertheless, the overriding focus should be to obtain diagnostic-quality images, particularly of the aortic root, whilst still following the principle of 'As low as reasonably practicable' (ALARP).<sup>7</sup> Current guidelines are for a tube potential of 100 kV for patients with a body mass index (BMI)  $\leq 30$  kg/m<sup>2</sup> or 120 kV for  $>30$  kg/m<sup>2</sup><sup>21</sup>; however, where scanning hardware allows, more aggressive tube voltage reduction can be achieved with 80 kV commonly used for BMIs  $<26$ – $28$  kg/m<sup>2</sup>.<sup>20</sup>

Traditionally patients receiving TAVI have often been in their eighth or ninth decades of life, with a mean age of 80–84 years in high/intermediate-risk trials.<sup>21–24</sup> Although this has fallen slightly in more recent low-risk trials, even in the PARTNER 3 trial, the mean age of recruited patients was 73 years.<sup>4</sup> Thus although radiation dose should be monitored, diagnostic image quality and contrast medium dose are arguably of greater concern.

### Imaging of the aortic root

As a minimum, the aortic root must be imaged, but the whole heart can be included to add information about the coronary arteries (either as part of a single scan or as a separate acquisition). ECG gating during acquisition is mandatory. The size of the aortic root is most frequently at its maximum during systole,<sup>25,26</sup> with the majority of industry THV sizing algorithms using systolic measurements. As a result, annulus measurements during diastole may lead to under sizing of THV.<sup>8,27</sup> As such, scanning of the aortic root should acquire systolic phase imaging. Infrequently, such as in the setting of septal hypertrophy, the aortic root is largest during diastole, as a result of which there is some benefit to the acquisition the full cardiac cycle.<sup>26,28,29</sup> Such acquisition is further meritorious as it provides multiple phases to work with to reduce the impact of motion artefact; however, such acquisition should be weighed against radiation and contrast medium concerns, particularly if high-pitch single-phase whole-body acquisitions are being performed.

#### *Aortic root: anatomical definitions and assessment*

The aortic root consists of the aortic annulus, sinuses of Valsalva, valvular cusps, fibrous interleaflet triangles, coronary artery ostia, and sinotubular junction.<sup>30,31</sup>

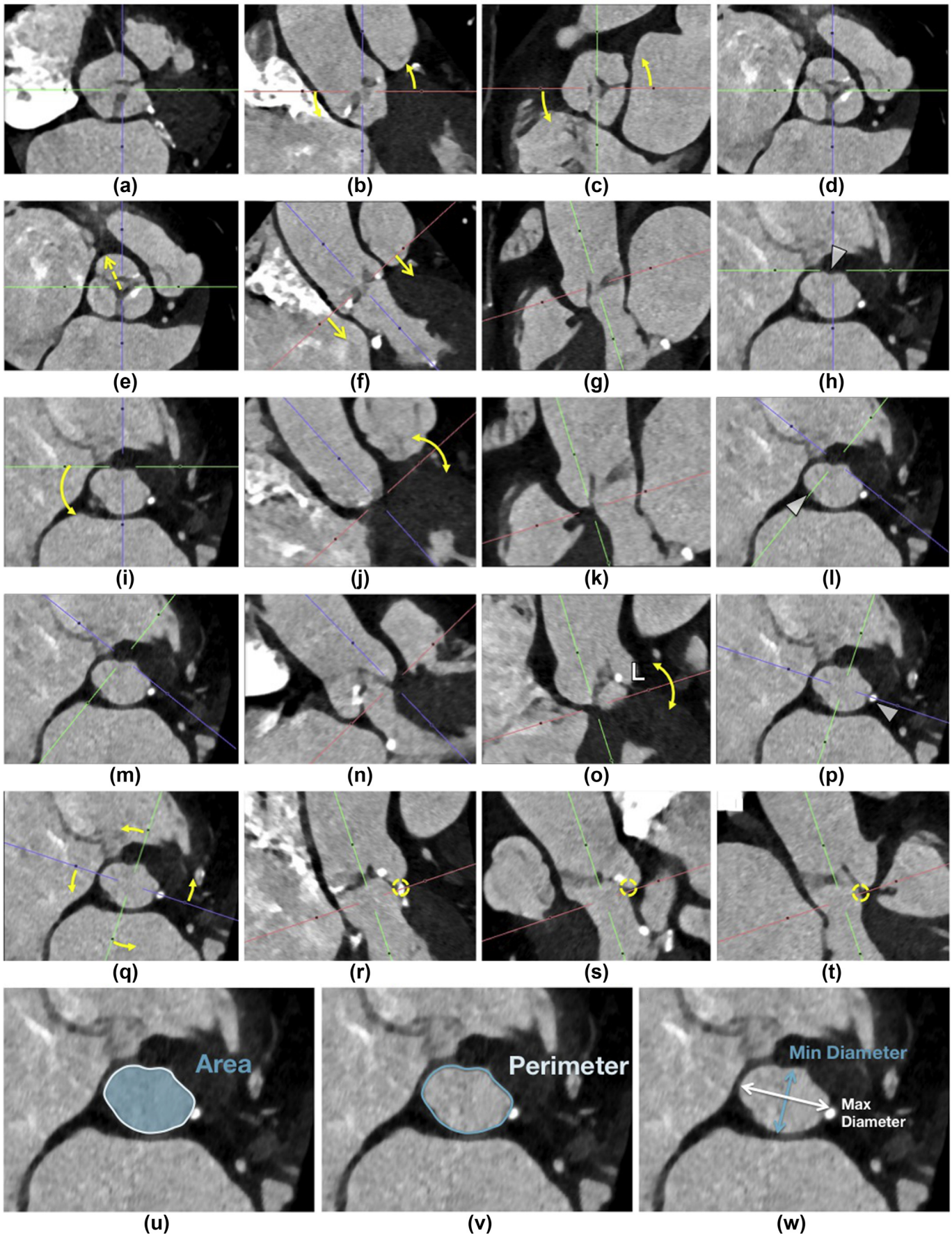
### Annulus

Accurate identification and planar analysis of the annulus is required for TAVI. Most commercially available software packages now facilitate identification of the aortic annulus automatically. User confirmation of the annulus is necessary, however, and as such, an understanding of the methods required to define the annulus is required, with the most commonly used technique being that of the sequential identification of each of the hinge points of the three cusps (Fig 2).

The perimeter, area, and diameter of the annulus are all important measures in THV sizing algorithms. Delineation of these should always be reviewed and corrected where necessary, as software-derived contours are not always accurate. In the presence of annular calcification, the annulus contour should be defined as to be harmonious with the rest of the annulus, running through the calcium in a manner that would best represent the annulus were the calcification absent.

Aortic root and annulus dimensions vary throughout the cardiac cycle<sup>24</sup>; with the annular area being more sensitive to changes during the cardiac cycle than perimeter.<sup>25</sup> The annulus is usually largest during systole and should therefore ideally be measured during this phase, although where the full cardiac cycle acquisition has been performed, a review of the whole cardiac cycle should be performed to confirm this is the case. Currently available software for semi-automated analysis will usually only measure and extract a single pre-selected cardiac phase, potentially limiting its role in this assessment of the cardiac cycle. There are early reports of full cycle segmentation following the manual identification of the hinge points allowing for a more rapid assessment of cyclical annular deformation and identification of the phase with the largest area.<sup>32</sup> Such advancements will be further bolstered in the future by advances in the automatic identification and segmentation of the aortic root.<sup>33,34</sup>

In the future we may be able to progress beyond matching annular sizing to industry provided sizing recommendation charts to a bespoke model utilising patient-specific computational flow dynamic (CFD) models. Through the use of deformable models and simulated THVs, the impact of the THV on the native geometry can be assessed.<sup>35</sup> To date such models have been shown to be accurate in their prediction of the degree of annular stretch and displacement and deformation of both leaflets and left ventricular outflow tract.<sup>36</sup> Such modelling has in turn allowed for the accurate prediction of the severity and location of paravalvular leakage by identifying regions where the presence of calcium may result in loss of contact between the annulus and the adjacent stent.<sup>37,38</sup> Furthermore, by quantifying the level and force of contact of the deployed valve against the membranous septum, the likelihood of damage to the conduction system and subsequent requirement for pacemaker has been predicted with high accuracy.<sup>39</sup> Future work is required to test the impact of this information on outcomes in prospective studies.



## Valve type

Characterisation of valve type (i.e., true or functional bi, tri, or quadri-cuspid) should be performed on all TAVI CT. Although in current clinical cohorts, predominantly composed of septuagenarians and octogenarians, tricuspid valve morphology is the most commonly encountered, bicuspid valves still account for 6–8% of patients presenting for TAVI.<sup>3,40</sup> With reducing cohort age, such as seen in the most recent low-risk trials, the frequency of bicuspid aortic valves presenting for consideration is likely to increase. Bicuspid valves reduce the success rates for TAVI (85.3% versus 91.4%)<sup>41</sup> with consequent higher conversion rate to surgery (2% vs 0.2%). Recognition and communication of the bicuspid valve nature is therefore important, especially as bicuspid valve morphology can be overlooked in >50% of cases based on echocardiography alone.<sup>42</sup>

Although numerous bicuspid aortic valve morphology classifications exist, a TAVI-centred classification has been created.<sup>43</sup> This categorises bicuspid aortic valve morphology based on whether there are two or three commissures and the presence/absence of a raphe. This divides bicuspid aortic valves into three types: (1) functional/acquired tri-commissural, (2) bi-commissural with raphe, and (3) bi-commissural without raphe.

Valve morphology and associated findings should always be reported. Valve calcification should be quantified and qualified.<sup>41</sup> Raphe position (between which leaflets) and length should also be noted.<sup>44</sup> Bicuspid aortic valve disease is part of an aortopathy and the ascending aorta, arch and descending aorta should be carefully inspected, with dilation, aneurysms and coarctation all more common in bicuspid valve disease. An additional challenge with bicuspid aortic valve disease is the definition of the annulus and annular plane, given that only two points of reference exist in the bi-commissural type valves. A schematic for overcoming such limitations, based on the traditional annular sizing approach, is provided in Fig 3. Although such measurements are highly reproducible, further work in optimising pre-procedural sizing is required in bicuspid valves; post-procedural imaging shows deployed TAVIs to be under-expanded by 11% relative to the native annulus, in contrast to devices deployed in tricuspid valves, which usually reach their expected dimensions.<sup>45</sup>

## Calcific burden

THV are deployed in specific landing zones, defined by the distal left ventricular outflow tract (LVOT), aortic

annulus, and valve cusps.<sup>46,47</sup> The degree of calcification within this landing zone varies with patients, with severely stenotic valves often yielding Agatston scores in excess of 2,000. There is also variance in the regions of the landing zone most afflicted, with non-coronary and left coronary cusps more frequently calcified. Sub-annular calcification presents a risk of paravalvular regurgitation, especially if the morphology of the calcium is more protruding than eccentric.<sup>48–52</sup> Balloon expandable valves are at increased risk of rupture with large protruding calcifications, and self-expanding valves should be considered in these situations.

At present, evaluation of landing zone calcification is non-quantitative, with anatomical distribution, protruding versus non-protruding calcifications noted, with a visual score of mild/moderate/severe assigned (Fig 4).<sup>6</sup>

## Optimal projection curves

TAVI CT can be used to plan optimal C-arm angulations, i.e., angulations that present the axis of the aortic root parallel to the fluoroscopic detector (Fig 5). These predictive angulations correlate well with the final procedural c-arm angles and more importantly, reduce procedural time and volume of contrast medium administered.<sup>53–63</sup>

Often, views with LAO 10 are the result, and an institutional preference should be clarified, and should be reported with their corresponding cranial or caudal angulation (Fig 5). When extreme angulation (>30°) is required to achieve these, alternate angulations should be provided; however, it is essential to recognise that CT predicted angles are only helpful if the patient is positioned in a similar fashion during CT and the TAVI procedure.

## Prediction of risk

For surgical aortic valve replacement, the Society of Thoracic Surgeons score (STSS) is the reference standard for the prediction of operative risk.<sup>64</sup> In TAVI, where the procedure itself is minimally invasive, the traditional risk assessment is supplemented by CTA. Through the individualised anatomical assessment provided by the CTA, a personalised risk of complications can be identified. Through the identification of specific CT features, the risk of coronary occlusion, annular rupture, paravalvular leakage, conduction disturbances, and vascular injury can all be predicted.

**Figure 2** Defining the annular plane. The annular plane is created by localising the three hinge points of the three valve cusps. This can be done in a standardised and reproducible manner using the following technique. First, an approximate plane is defined through the aortic valve (a–d). The centre of the cursor should then be located over the right coronary cusp (RCC) hinge point scrolling down until the hinge disappears (e–h). This is now one of the three hinge points defined, and this annular point should remain fixed until the remaining two points are identified. The second plane is then rotated so that it transects the location of the non-coronary cusp (NCC) (i) and then angled (j) until the NCC cusp hinge point disappears, just as the RCC did in the previous step (arrowhead, i–l). Now two of the three planar points are fixed, and the only thing that should now be moved or rotated is the third plane (note no movement in (g) or (k) during the previous steps). This third plane (o) should now be angled until the third hinge point disappears (m–p). The three hinge points are now fixed in place. To confirm the accurate placement of these (often required in heavily calcified annuli and cusps), the cursor can now be centred in the annulus and the view rotated (q), so that each of the three hinge points can be visualised in turn (yellow dashed circles, r–t). Once these hinge points are confirmed, the annular area and perimeter can be measured (u–w).

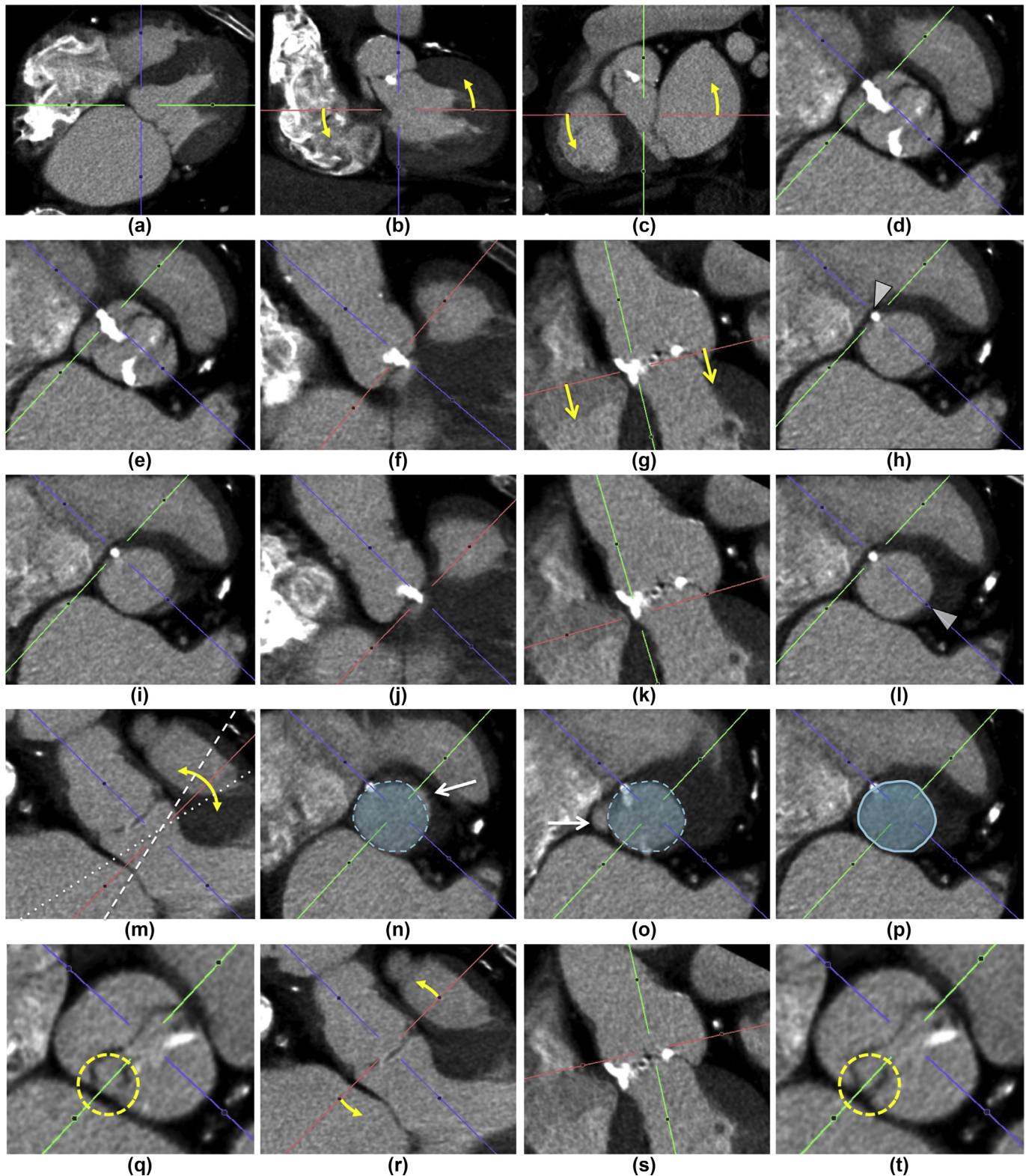


**Figure 3** Annulus definition in bicuspid aortic valves. First an approximate aortic root plane is defined (a–c) with the cursor centred over the middle or raphe of the cusp in the approximate right coronary cusp position. Once this is centred and the cusps appear relatively symmetrical, the image is scrolled down (e–g) until the hinge point of this cusp is reached (arrowhead, (h)). The plane that transects the second hinge point (k) is then angled, until the second hinge point is reached (arrowhead, (l)). Two techniques can then be used to define the final annular plane: the plane orthogonal to the plane transecting the hinge points (m) can be angled, until the smallest short axis diameter is achieved (p). Over- and under-angulation results in greater diameters (arrows in (n) and (o)) demonstrating the appearance of a wider annulus with angulation compared with the minimal diameter achieved in (p). Alternatively, the image can be scrolled up to the commissures of the bicuspid valve (q) and the plane going through these (r) angled until they are both symmetrical (note the wider commissure circled in (p)), which becomes closed and symmetrical with the opposite commissure as circled in (t).



**Figure 4** A semi-quantitative approach to LVOT calcification. In mild calcification, the calcification is lamellated along the annular wall, non-protruding and small in size. In moderate cases, there are multiple nodules of calcification or a single nodule with limited protrusion. In severe calcification, the nodule is large and protruding with extension into the LVOT or protruding with multiple nodules of calcification.



**Figure 5** MPR planes for optimal projection curve. The coronal–oblique plane passes through the NCC and left coronary cusp hinge-points while the sagittal oblique plane passes through the RCC hinge-point. This produces a viewpoint of the three cusps centred on the right coronary cusp with all equidistant from one another: optimal for stent deployment.

### Annular rupture

Annular rupture occurs in only 0.1% of TAVI procedures; however, it has a mortality of up to 75% when an uncontained rupture arises.<sup>65,66</sup> It is increased by both patient related and procedural related factors. Prior radiotherapy, female gender, sub-annular calcification (especially inferior to the non-coronary cusp, and in the upper LVOT <2 mm below annular plane) all increase the risk. Procedural factors of THV oversizing >20%, and balloon-expanding valves all increase the risk.<sup>46,66</sup> Forearmed with the knowledge that the annulus is hostile and at risk of rupture through the

identification of subannular calcification and its location means that the procedure can be modified. Either through the use of self-expanding valves, or alternately through the use of reduced over sizing of valves, with this especially pertinent where an annulus sits in the grey zone between two potentially viable THV sizes.

### Coronary occlusion and sinotubular junction injury

One of the most feared complications of TAVI is that of coronary occlusion. Although rare, at 0.7% of all TAVIs, there is significant mortality when it occurs with a 41% 30-day

mortality.<sup>67,68</sup> Coronary occlusion is usually the result of an imbalance between the size of the THV and native aortic root, leading to occlusion of the coronary ostium. Determination of the coronary ostial height and sinus of Valsalva diameter is therefore mandatory on pre-procedural TAVI CT. All measurements are relatively straightforward (a schematic is shown in Fig 6, with a high-risk anatomy example in Fig 7): (1) coronary ostial height: after establishing the annular plane, the ostial height is determined perpendicular to the annular plane. Ostial heights of <12 mm carry an increased risk of post-implant coronary occlusion<sup>67</sup>; however, are not absolute contraindications; (2) sinuses of Valsalva: diameters measured on an in-plane en-face view, either cusp to cusp or cusp to commissure. For bicuspid valves, cusp to cusp is measured. The final figure is the average of all three measurements, with <30 mm considered higher risk<sup>67</sup>; and (3) sinotubular junction: the distance from annulus to the sinotubular junction and sinotubular junction planar diameters should also be

measured. Comparison between expected THV length and sinotubular junction height is necessary to avoid injury post implantation when there is a small diameter.

The combination of a low coronary height and a narrow sinus indicates a geometry that is at particular risk of subsequent coronary occlusion, although it should be noted that 13% of cases will have this anatomy with only a small subset experiencing obstruction.<sup>67</sup>

#### Paravalvular regurgitation

Paravalvular (annular) regurgitation (PAR) is an important cause of mortality after TAVI, with a greater than twofold increase in 1-year mortality in those with moderate to severe PAR.<sup>69–71</sup> Although procedural factors, such as device malpositioning (excessive aortic or ventricular positioning), are relevant, anatomical factors detected by CT are major determinants of PAR. These factors include device under-sizing,<sup>32,72</sup> root angulation,<sup>73</sup> and excess landing

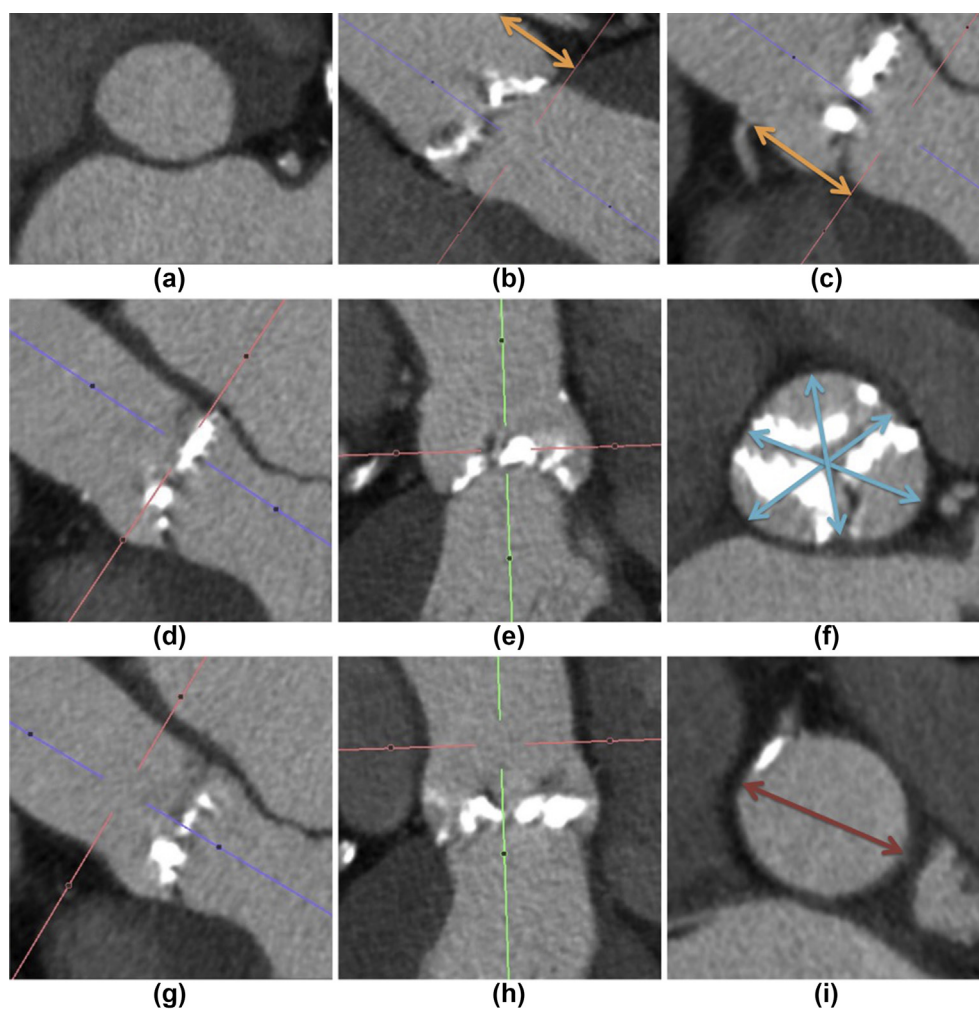


**Figure 6** Schematic for the measurement of coronary artery height (a–c), sinus of Valsalva diameter (d–f) and sinotubular junction diameter (g–i). For measurement of the coronary heights, the annular plane is first defined (a) and remains static. The coronary height is measured perpendicular to the annular plane (red line in (b) and (c)) to obtain the left coronary height (b) and right coronary height (c). The sinus of Valsalva diameter is measured at the widest diameter within the sinuses (d, e), with the three cusp to commissure distances measured (f). The final reported value is the average of these three. The sinotubular diameter is then measured at the junction between the sinus and aorta (g, h) with a single diameter measurement performed at this site (i).

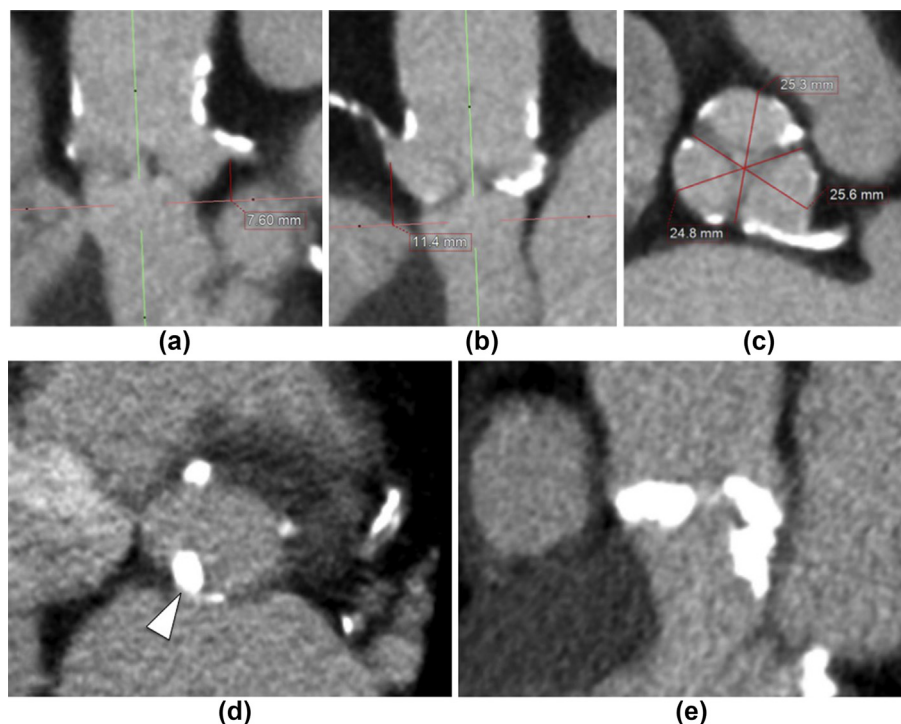


**Figure 7** High-risk anatomical features for TAVI insertion. (a–c) demonstrate low coronary ostial heights on the left (a), and right (b) as well as a small sinus (c). In (d) and (e) there is a large volume of nodular protuberant calcification below the non-coronary cusp (arrowhead) placing this patient at increased risk for paravalvular regurgitation and annular rupture.

zone calcification (both annular and left ventricular outflow tract calcification).<sup>48–51</sup> Bicuspid valve morphology has also been reported to be associated with increased rates of PAR,<sup>74,75</sup> although this appears to be much less of an issue with the most recent generation of valves.<sup>42,76,77</sup>

#### Conduction disturbances

Significant advances in TAVI design in conjunction with improved patient selection and risk prediction using CTA have led to a substantial reduction in the incidence of procedural complications over the last decade.<sup>65</sup> One complication that persists despite these advances is post-procedural conduction disturbance requiring pacemaker implantation, which in a recent meta-analysis of 10,822 cases remained high at 16.2% of cases. Assessment of the length of the semi-membranous septum may be a useful marker in the identification of patients at risk of this complication, allowing for targeting of preventative treatment or alteration of procedural strategy. The membranous septal length is measured in the coronal plane, at the longest point between the cusp hinge point and the muscular septum, with a length <8 mm predictive of high-degree atrioventricular (AV)-block post-TAVI.<sup>78</sup> Several subsequent studies have confirmed this observation, and additionally, demonstrated the additive deleterious effect of calcification of the landing zone, particularly when located beneath the left coronary cusp.<sup>79–81</sup> Such features provide additive incremental risk over and above the clinical and procedural risk factors of deep implant depth, and pre-

existing right bundle branch block.<sup>80,81</sup> Highlighting the length of the membranous septum can, in turn, allow the interventionist to alter the implantation depth of the valve to prevent damage to the conduction system. Such an approach has been shown to reduce the rate of PPM insertion from 10% to 3%.<sup>82</sup> Knowledge of these anatomical and procedural markers of risk may in future lead to new valve designs to mitigate this. One such valve design was the Centara valve (Edwards Lifesciences, Irvine, CA, USA), which had a fixed implant depth due to the combination of a waist, sinus bulge and flared LVOT component. Early trials validated this concept of a fixed implant depth with 1 year outcomes from this valve showing rates of PPM insertion of only 5%.<sup>83</sup> Although this valve has subsequently been withdrawn from development due to issues with device tracking and manipulation, it provides a powerful proof of concept of translating research findings into actionable outcomes. Such advances in design combined with knowledge of the differing risk profiles of both individual patients and devices may in the future allow for targeted device selection to best address the patient specific risk profile as quantified by their CTA.

#### THV delivery route and vascular assessment

Although understanding of the aortic root is fundamental to deployment of a transcatheter aortic valve, appreciation of the vascular access is also mandatory for optimal delivery of the device. At present, the transfemoral route is usually the first route of choice<sup>84,85</sup> and the

approach with the most experience worldwide.<sup>86</sup> The PARTNER2 and SURTVAI trials demonstrated a major vascular complication rate of up to 6%<sup>23,87,88</sup> with risk factors for major vascular complications being identified as increased vessel tortuosity, increased calcification, and insufficient vessel diameter. Initial devices had a cut-off external THV sheath:vessel diameter ratio of  $\geq 1.05$ ; however, newer evidence suggests a threshold of  $\geq 1.12$  can be used, particularly in the absence of severe calcification.<sup>89</sup>

Alternative approaches are required when the transfemoral approaches are contraindicated.<sup>86</sup> The original approaches included trans-apical and direct trans-aortic. The trans-subclavian approach has migrated from a surgical to percutaneous approach, with the left-side access favoured, although the trans-carotid approach requires minimally invasive surgery, with the left carotid again favoured due to favourable alignment with the ascending aorta.<sup>90–92</sup> The most recent approach being explored is that of the trans-caval approach, with crossover into the abdominal aorta in the retroperitoneum.<sup>93</sup> This technique remains experimental, however, and has stringent abdominal anatomy requirements including a suitable calcium-free window in the aorta in a position where it directly apposes the vena cava, and necessitates the use of a post-procedural occluder device.

The vascular CT angiogram should be carefully assessed for suitability, primarily for transfemoral route access, and if not suitable, also for trans-carotid and trans-subclavian routes. This can easily be achieved manually with double-oblique views on multiplanar reformats. Semi-automated evaluation with post-processing algorithms facilitates easier evaluation, with curved multiplanar reformats well suited to this task.

Access routes should be assessed for the calcium severity. Special note should be made of obvious luminal protrusions and circumferential/near-circumferential calcification, particularly at bends and bifurcations. These may limit vessel elasticity, and therefore, the ability to accommodate the transiting deployment sheath.

Knowledge of the tortuosity of the vasculature is also vital. Although most bends can be navigated with the deployment sheath, with limited risk of damage, acute angles and heavily calcified tortuous vessels present a greater challenge. The minimum vessel diameters should be evaluated and reported for each segment from common femoral/subclavian/common carotid artery to the aortic root. All vasculature should be assessed for additional pathologies, including but not limited to: aneurysm, dissection, tethering, and focal stenosis. The intended access sites should be assessed for any variant anatomy, such as high bifurcation of the common femoral artery or heavy calcification anteriorly at the expected puncture site.

## Coronary artery assessment

Coronary artery disease (CAD) is common in those undergoing TAVR, with >60% of patients having at least one vessel with >70% stenosis.<sup>22,23</sup> Although management of

CAD remains controversial, good procedural success is reported, and identification of this beforehand can allow for appropriate discussion with the patient.<sup>94</sup> With improving spatial and temporal resolution as well as broader z-axis coverage, modern CT systems can visualise the coronaries with diagnostic image quality. This is especially true for the assessment of coronary artery anatomy anomalies. Full diagnostic quality, in those with contraindications to usual practice, however, is challenging due to multiple factors. As part of patient preparation, nitrates are contraindicated, reducing coronary artery dilation that would normally be present in a CTA. Often, those necessitating TAVI have high coronary calcific burden further reducing the confidence of the reporter.<sup>95</sup> Despite these limitations, a high negative predictive value can often be achieved.<sup>96</sup> Limiting the reporting of CAD in TAVI patients to only those with “high-risk” CAD (two-vessels with  $\geq 50\%$  stenosis with involvement of the proximal left anterior descending [LAD] artery, or three-vessels with  $\geq 50\%$  stenosis, or left main with  $\geq 50\%$  stenosis) may be more appropriate in the TAVI/TAVR population given the higher age, background burden of disease, and limited evidence of significant benefit of concomitant/preprocedural percutaneous coronary intervention (PCI) for incidentally detected CAD in this group.<sup>97,98</sup> Use of such a threshold reduced the number of positive CTA examinations from 41% to 11% in one study.<sup>95</sup> Reporting of CAD may nonetheless be useful in appropriately selected patients (younger, sinus rhythm, low calcium burden) with the potential to reduce the need for a separate diagnostic angiogram. Given the challenge of rate control end-systolic CTA may be more appropriate in this cohort of patients.

## Holistic care

As with any radiographic imaging technique, it is paramount that all acquired data are thoroughly assessed for relevant and incidental clinical findings. The CT dataset available for TAVI is effectively a CT examinations of the neck/chest/abdomen/pelvis with an additional ECG-gated cardiac set. The whole wide field of view acquired should be reviewed as normal by a trained radiologist. The long-term consequence of missed findings is becoming more relevant as the mean cohort age for TAVI reduces.<sup>4</sup> Nineteen to 20% of TAVI work-up examinations have incidental potentially malignant findings.<sup>99,100</sup> These incidental findings are potentially significant, and are associated with poorer survival than in those without incidental findings.<sup>99</sup> Importantly though, if these findings are detected and addressed in concert, with their TAVI triaged accordingly to best facilitate ongoing care, the differences in survival between those with and without significant findings becomes negligible.<sup>100,101</sup>

## Post-procedural follow-up and assessment

The main imaging method to follow-up TAVI is that of echocardiography.<sup>102,103</sup> CT imaging provides a useful adjunct in the follow-up period post-TAVI for problem-

solving, providing information about the THV geometry, position, and leaflet assessment.<sup>104–113</sup> In clinical scenarios where there is clinical concern for infective endocarditis, valve thrombosis, or structural degeneration, that has not been confirmed/excluded on echocardiography, CTA of the root can provide useful ancillary information.<sup>9,85</sup>

Follow-up CT should focus on the aortic root and be of diagnostic quality for the entire cardiac cycle to allow for both anatomical and functional assessment. Imaging can be challenging due to streak, blooming, and motion artefacts from the metallic stent struts. Beta-blockers can be used to reduce heart rate and R-R variability and thus improve image quality where the transvalvular gradient is mild to moderate. The THV leaflets should be uniform in size and motion on the four-dimensional (D) CT dataset. Leaflet thickening or restricted movement, termed hypo-attenuated leaflet thickening or hypo-attenuation affecting motion, usually represent the formation of thrombus or pannus (Fig 8).<sup>114–118</sup> CT attenuation is a useful adjunct in the assessment of perileaflet thickening with <145 HU suggestive of thrombus rather than pannus.<sup>119</sup> Due to the relatively low temporal resolution of CTA, maximal leaflet opening may be missed, occurring in between the captured phases. As a result, and given the implications for treatment, restricted motion should be reported with caution in the absence of leaflet thickening.<sup>116,118,120</sup>

### Valve–In–Valve implantation

TAVI valve-in-valve (VIV) implantation within failing existing surgical bioprosthetic valves has demonstrated promise with a high technical success rate, an 83–100% 30-day survival with symptomatic outcomes of New York Heart Association (NYHA) class of I/II achieved in 89–100%.<sup>121</sup> Maintenance of good technical results have been demonstrated out to 3 years, and the indications for this are likely to grow with time.<sup>122</sup>

The Valve-In-Valve International Data (VIVID) registry shows a 2.3% risk of coronary occlusion in valve in valve implants, compared with 0.66% for native valve TAVI.<sup>67,123</sup> This increased rate is due to three factors: firstly, the

surgical valve leaflets are a continuous sheet of pericardium, meaning that when forced open they form a tube pinned between the original surgical valve and the newly implanted TAVI; secondly, the aortic root dimensions are frequently small with a reduced height between the neo-annulus and the coronaries; and third, the position of the existing implanted prosthetic heart valve (IPHV) can be asymmetrically sited so as to be canted towards one of the ostia.

Implantation of a THV within a pre-existing surgical valve brings several new challenges in pre-procedural planning. The native annulus is no longer the narrowest point in which the new TAVI valve will now anchor itself, with this now defined by the neo-annulus of the IPHV, which may be elevated in position compared to the native annulus. IPHV are comprised of surgical (stented versus stentless) and THV. In a stented IPHV, the bioprosthetic leaflets are forced into a perpetual open position forming a cylinder. This cylinder prevents flow through the mesh of the new TAVI and fixes the orientation of the aortic root. This orientation may deviate significantly from perpendicular to the sinotubular junction. Given this altered orientation, there is increased possibility of coronary ostia occlusion. A method to evaluate the altered orientation proposed is the virtual THV to coronary distance.<sup>124</sup> This is designed to predict the distance of the new implanted THV frame from the coronary ostia. It is based on a comparison of the predicted outer circumference of the IPHV compared with the coronary ostia. A threshold of 4 mm has a high accuracy for the prediction of coronary occlusion with an area under the curve of 0.94;<sup>123</sup> however, this of course means that some with a shorter distance will go unoccluded, although some with a greater distance will occlude. Thus a more granular range of values can also be considered where <3 mm is high risk, 3–6 mm intermediate, and >6 mm low. A schematic for the assessment of the surgical valve replacement is provided in Fig 9, with examples of high-risk features in Fig 10.

The CT TAVI for a VIV should be the same as for standard TAVI, with at minimum an ECG-gated aortic root dataset and vascular CT angiogram. If the neo-annulus of the IPHV is

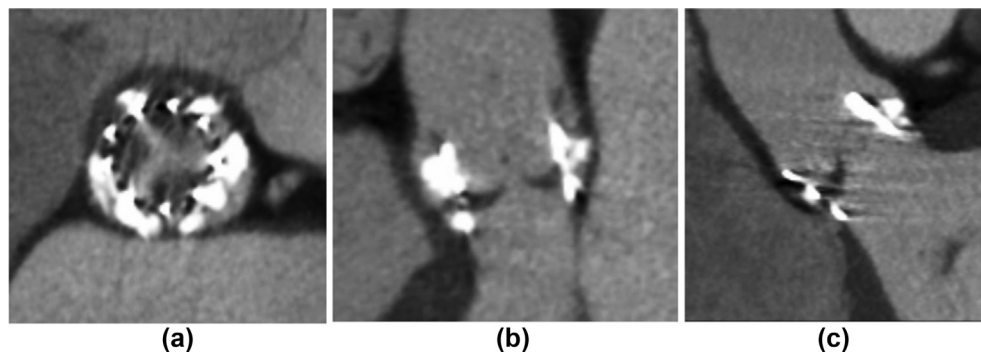


**Figure 8** Hypo-attenuated leaflet thickening (HALT) in a Sapien XT valve showing three leaflet thrombosis on the short axis (a) as low attenuation centred on the middle of each of the three leaflets, and on the long axis view (b and c) as meniscal low attenuation thickest at the hinge points. This involves >75% of the leaflet length of all three leaflets.

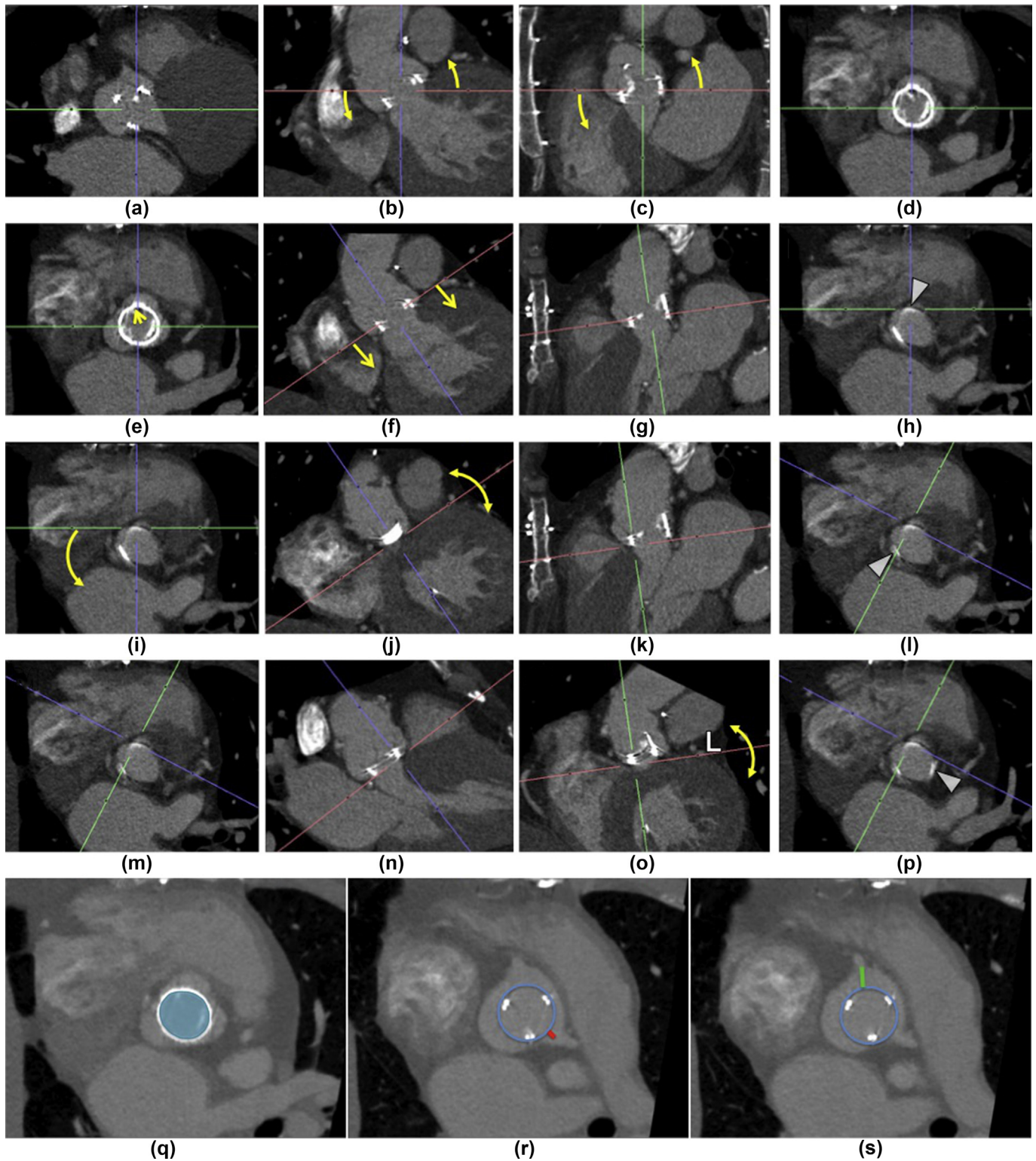


**Figure 9** Aortic VIV assessment with calculation of virtual transcatheter to coronary ostia distances. As with assessment of the native aortic valve an annular plane needs to be defined. This is done using the three most basal points of the surgical aortic valve basal ring. First, an approximate aortic plane is described (a–d). Following this the image is centred on the most basal point of the undulation in the RCC position (e–h). The most basal point of the undulations in the approximate NCC and LCC position are then identified in the same way as the native aortic valve (i–p). Based on the known valve size or based on the valve area and internal diameter (q), a virtual transcatheter valve is then simulated within the surgical valve (r–s) from which the distances between this and the coronary ostia can be measured.

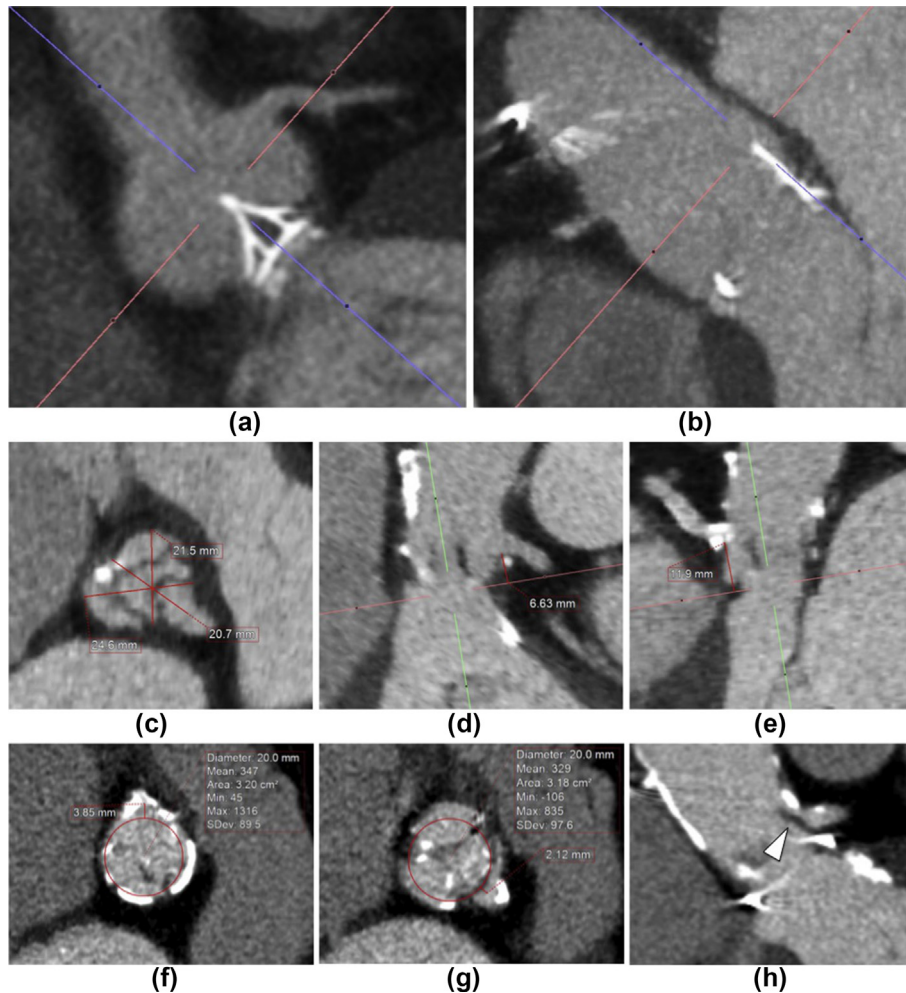


**Figure 10** Examples of low- and high-risk coronary anatomy in patients undergoing VIV work-up. In (a) and (b) the coronaries arise above the uppermost extent of the surgical stent struts eliminating the risk of procedural related coronary occlusion. In (c–e) a patient with a stentless surgical aortic valve has a distorted root with very low coronary arteries, and a small Sinus of Valsalva placing them at high risk of occlusion. In (f) and (g) the virtual transcatheter heart valve to coronary ostia distances are small bilaterally, with (h) demonstrating the impending occlusion of the left main by the adjacent leaflet (arrowhead) should a TAVI be inserted.

not specified in the patient medical records, this can be estimated on CT.<sup>125</sup> CT allows for demonstration of the inner valve area and an effective diameter, in a method similar for native annulus. Reference charts are available; however, they do not cover the complete range of available THVs, or indeed previously implanted surgical valves.<sup>125,126</sup>

#### TAVI-in-TAVI

Due to the combination of the limited time over which TAVI has been performed, and the historical high burden of comorbidities in those that received TAVI, the frequency with which degenerate TAVIs are encountered is low<sup>127</sup>; however, as TAVI becomes more commonly performed in lower-risk groups, degenerate TAVI valves will become more commonplace. Re-do TAVI within the first TAVI has been shown to be an effective therapy with favourable short- and medium-term outcomes.<sup>128</sup> Currently, data are extremely limited on risk markers for risk of coronary obstruction in TAVI-in-TAVI. In the largest case series to

date, coronary occlusion occurred in one case (2% of total cases) secondary to native leaflet displacement during valve deployment.<sup>128</sup> The mechanism of the risk of coronary occlusion in TAVI-in-TAVI is likely similar to that of VIV, with the initial TAVI leaflets being held open creating a covered stent within the root. Thus until more substantive evidence is available, it is reasonable to approach these in a similar manner to VIV, with the use of the VTC technique. The second stent to be inserted will be of the same size as the initial TAVI device; however, TAVI expansion is frequently incomplete.<sup>45</sup> Thus the native TAVI should not be used as the marker for measuring VTC, and the theoretical maximum expansion should be used in the VTC measurement. Systolic imaging to ascertain the height of the open leaflets is beneficial, as unlike SAVR, the stents do not offer a useful surrogate marker of leaflet height in TAVI devices. Additional attention must be paid to the risk of sinus seal-off, especially in self-expanding valves as their supra-annular leaflet position and long skirt all bring the valve closer to the StJ and increase the possibility of complete

circumferential sealing in those with small sinuses and a low sinotubular junction.

## Post-TAVI coronary intervention

The incidence of progression of the underlying CAD and need for subsequent post-TAVI PCI is poorly understood at present. Despite a high prevalence of obstructive CAD pre-TAVI, the need for post procedural intervention was only 3% in one study of 1,000 TAVIs inserted.<sup>129</sup> In those who do require PCI, the TAVI device presents a significant hurdle to the performance of procedure, with stent struts frequently overlying the access route for coronary ostial engagement.<sup>130</sup> Outside of the acute setting where direct progression to ICA is recommended, CTA can play a useful role in the work-up of the cause of angina post-TAVI. Although the challenge of a high calcium burden remains post-TAVI, beta-blockade and glyceryl trinitrate can be safely administered, improving the visualisation of the coronary arteries. The most common cause is progression of the original CAD; however, delayed coronary obstruction secondary to the TAVI implantation can occur months after the initial valve insertion.<sup>131</sup> As with acute occlusions, low coronary heights, and a narrow sinus of Val-salva are risk factors, with valve-in-valve procedures, neo-sinus and native leaflet thrombus and fibrous endothelialisation posited to be further risk factors for delayed obstruction.<sup>131</sup> CTA can also be used to map out the procedural approach, examining the location of the stent struts, upper margin of the TAVI skirt, and the position of the native aortic leaflet in relation to the coronary ostia.<sup>130</sup> For the latter, partial leaflet compromise of the coronary ostium has been reported in up to 42% of cases, more frequently on the right than left.<sup>132</sup>

## Report generation

Screenshots with the required measurements should be stored with the patient CT TAVI DICOM dataset for quick reference on the PACS system. These include aortic annulus dimensions, aortic root dimensions, coronary ostial heights, vascular approach (as either 3D volumes or 2D centreline images). A suggested standardised report proforma is provided in Table 1. A report combining screenshots or line drawings with the measurements obtained from CT can make for a more intuitive and easily understood summary, which can more readily be incorporated into the catheter laboratory environment. Where local software permits, such an approach is salutatory.

A mechanism should be present to allow for the discussion of TAVI cases, particularly when adverse imaging features are present. Cardiac imagers should feel empowered to highlight adverse features and their prognostic implications. Such features may not alter whether a TAVI is conducted; after all, many of these patients are of high- or prohibitive-surgical risk such that no alternative treatment strategies are available; however, prior knowledge of risk can allow for mitigating steps to be undertaken. These can range from changing of the valve type being used, such as using a self-expanding valve in a root anatomy at risk of

**Table 1**  
Suggested reporting template for reporting of TAVI work-up studies.

CT TAVI
COMPARISON:
FINDINGS:
GENERAL:
Levocardia
Conventional drainage of the SVC, IVC and coronary sinus
Conventional pulmonary venous drainage into the left atrium
Left aortic arch, with normal branching pattern
AORTIC VALVE AND ANNULUS:
___ Trileaflet valve
___ Severe aortic valve calcification (aortic valve calcium score: ___AU).
The annulus during ___systole/___diastole (phase ___%) measures:
Area: ___ (mm <sup>2</sup> ).
Perimeter: ___ (mm)
Left coronary height: ___ (mm)
Right coronary height: ___ (mm)
Sinus: ___ (mm)
Sinotubular junction height: ___ (mm).
Sinotubular junction diameter: ___ (mm)
LVOT calcification is ___absent/___present.
The estimated deployment angle is ___°
ABDOMINAL AORTA:
The abdominal aorta and major branches (coeliac axis, superior mesenteric, renal, and inferior mesenteric arteries) are intact
Pelvic vessels (internal and external iliac arteries) are intact
Right iliofemoral arteries measure ___ (mm) in minimum diameter, without significant tortuosity, calcification, or narrowing
Left iliofemoral arteries measure ___ (mm) in minimum diameter, without significant tortuosity, calcification, or narrowing
(If iliofemoral access is not feasible):
Right subclavian artery measures ___ (mm), without significant tortuosity, calcification, or narrowing
Left subclavian artery measures ___ (mm), without significant tortuosity, calcification, or narrowing
Patent right common carotid artery measures ___ (mm) minimum diameter, without significant tortuosity, calcification, or narrowing
Patent left common carotid artery measures ___ (mm) minimum diameter, without significant tortuosity, calcification, or narrowing
Patent right vertebral artery
Patent left vertebral artery
CARDIAC FINDINGS:
Cardiac chambers are normal in size
Right dominant coronary system
___ Extensive triple vessel coronary artery calcifications are seen
No proximal obstructive coronary artery disease
EXTRACARDIAC FINDINGS:
No significant extra-cardiac findings
IMPRESSION:
Severe aortic valve stenosis with the annulus measurement during ___systole/___diastole (mm)
The cross-sectional area of the annulus during systole is ___ (cm <sup>2</sup> ).
The perimeter during systole is ___ (mm).
___ Femoral access suitable.

rupture, wiring the coronaries prior to commencement of TAVI deployment if at high risk, through to performing the procedure in a hybrid theatre to minimise occlusion to revascularisation times should an occlusion occur.

## Summary

For surgical aortic valve replacement, the Society of Thoracic Surgeons score (STSS) is the reference standard for

the prediction of operative risk. In TAVI though, where the procedure itself is minimally invasive, the traditional risk assessment is supplemented by CTA. Through a consistent approach to the acquisition of high-quality images, and the standardised reporting of annular measurements and adverse root and vascular features, patients at risk of complications can be identified. In turn, this may allow for a personalised procedural approach and treatment strategies devised to potentially reduce or mitigate this risk.

## Conflict of interest

The authors declare the following financial interests/personal relationships which may be considered as potential competing interests: JL serves as a consultant and has stock options in HeartFlow and Circle Cardiovascular Imaging and receives speaking fees from GE Healthcare. He also provides core laboratory services to Edwards Lifesciences, Abbott and Medtronic through institutional agreements EN has served as a consultant to GE Healthcare and has received speaker fees from GE Healthcare and Siemens. AYF, and JWM have no relevant disclosures.

## References

- Cribier A, Eltchaninoff H, Bash A, et al. Percutaneous transcatheter implantation of an aortic valve prosthesis for calcific aortic stenosis: first human case description. *Circulation* 2002;**106**(24):3006–8. <https://doi.org/10.1161/01.CIR.0000047200.36165.B8>.
- Leon MB, Smith CR, Mack M, et al. Transcatheter aortic-valve implantation for aortic stenosis in patients who cannot undergo surgery. *N Engl J Med* 2010;**363**(17):1597–607. <https://doi.org/10.1056/NEJMoa1008232>.
- Popma JJ, Deeb GM, Yakubov SJ, et al. Transcatheter aortic-valve replacement with a self-expanding valve in low-risk patients. *N Engl J Med* 2019;**380**(18):1706–15. <https://doi.org/10.1056/NEJMoa1816885>.
- Mack MJ, Leon MB, Thourani VH, et al. Transcatheter aortic-valve replacement with a balloon-expandable valve in low-risk patients. *N Engl J Med* 2019. <https://doi.org/10.1056/nejmoa1814052>.
- Achenbach S, Delgado V, Hausleiter J, et al. SCCT expert consensus document on computed tomography imaging before transcatheter aortic valve implantation (TAVI)/transcatheter aortic valve replacement (TAVR). *J Cardiovasc Comput Tomogr* 2012;**6**(6):366–80. <https://doi.org/10.1016/j.jcct.2012.11.002>.
- Blanke P, Weir-McCall JR, Achenbach S, et al. Computed tomography imaging in the context of transcatheter aortic valve implantation (TAVI)/transcatheter aortic valve replacement (TAVR): an expert consensus document of the Society of Cardiovascular Computed Tomography. *J Cardiovasc Comput Tomogr* 2019;**13**(1):1–20. <https://doi.org/10.1016/j.jcct.2018.11.008>.
- FitzGerald R, Smith K, Wilson D. A guide to understanding the implications of the Ionising Radiation (Medical Exposure) Regulations in diagnostic and interventional radiology. *R Coll Radiol* 2015 <https://www.rcr.ac.uk/publication/guide-understanding-implications-ionising-radiation-medical-exposure-regulations>. Last accessed 16/12/19.
- Clavel MA, Messika-Zeitoun D, Pibarot P, et al. The complex nature of discordant severe calcified aortic valve disease grading: new insights from combined Doppler echocardiographic and computed tomographic study. *J Am Coll Cardiol* 2013;**62**(24):2329–38. <https://doi.org/10.1016/j.jacc.2013.08.1621>.
- Baumgartner H, Falk V, Bax JJ, et al. 2017 ESC/EACTS guidelines for the management of valvular heart disease: the task force for the management of valvular heart disease of the European society of cardiology (ESC) and the European association for cardio-thoracic surgery (EACTS). *Eur Heart J* 2017;(September):1–53. <https://doi.org/10.1093/eurheartj/ehx391>.
- Pawade T, Clavel MA, Tribouilloy C, et al. Computed tomography aortic valve calcium scoring in patients with aortic stenosis. *Circ Cardiovasc Imag* 2016;**11**:e007146. <https://doi.org/10.1161/CIRCIMAGING.117.007146>.
- Abbara S, Blanke P, Maroules CD, et al. SCCT guidelines for the performance and acquisition of coronary computed tomographic angiography: a report of the society of cardiovascular computed tomography guidelines committee: endorsed by the North American society for cardiovascular imaging (NASCI). *J Cardiovasc Comput Tomogr* 2016;**10**(6):435–49. <https://doi.org/10.1016/j.jcct.2016.10.002>.
- Spagnolo P, Giglio M, Di Marco D, et al. Feasibility of ultra-low contrast 64-slice computed tomography angiography before transcatheter aortic valve implantation: a real-world experience. *Eur Heart J Cardiovasc Imag* 2016;**17**(1):24–33. <https://doi.org/10.1093/ehjci/jev175>.
- Annoni AD, Andreini D, Pontone G, et al. CT angiography prior to TAVI procedure using third-generation scanner with wide volume coverage: feasibility, renal safety and diagnostic accuracy for coronary tree. *Br J Radiol* 2018;**91**(1090):20180196. <https://doi.org/10.1259/bjr.20180196>.
- Mata-Mbemba D, Labani A, Ghannudi S El, et al. 320-row CT transcatheter aortic valve replacement planning with a single reduced contrast media bolus injection. *PLoS One* 2018;**13**(9):1–12. <https://doi.org/10.1371/journal.pone.0204145>.
- Pulerwitz TC, Khaliq OK, Nazif TN, et al. Very low intravenous contrast volume protocol for computed tomography angiography providing comprehensive cardiac and vascular assessment prior to transcatheter aortic valve replacement in patients with chronic kidney disease. *J Cardiovasc Comput Tomogr* 2016;**10**(4):316–21. <https://doi.org/10.1016/j.jcct.2016.03.005>.
- Bittner DO, Arnold M, Klinghammer L, et al. Contrast volume reduction using third generation dual source computed tomography for the evaluation of patients prior to transcatheter aortic valve implantation. *Eur Radiol* 2016;**26**(12):4497–504. <https://doi.org/10.1007/s00330-016-4320-8>.
- Mitchell JR, Schwartz CJ. Relationship between arterial disease in different sites. A study of the aorta and coronary, carotid, and iliac arteries. *Br Med J* 1962;**1**(5288):1293–301.
- Felmly LM, De Cecco CN, Schoepf UJ, et al. Low contrast medium-volume third-generation dual-source computed tomography angiography for transcatheter aortic valve replacement planning. *Eur Radiol* 2017;**27**(5):1944–53. <https://doi.org/10.1007/s00330-016-4537-6>.
- Martin SS, Albrecht MH, Wichmann JL, et al. Value of a noise-optimized virtual monoenergetic reconstruction technique in dual-energy CT for planning of transcatheter aortic valve replacement. *Eur Radiol* 2017;**27**(2):705–14. <https://doi.org/10.1007/s00330-016-4422-3>.
- Meyer M, Haubenreisser H, Schoepf UJ, et al. Closing in on the K edge: coronary CT angiography at 100, 80, and 70 kV—initial comparison of a second- versus a third-generation dual-source CT system. *Radiology* 2014;**273**(2):373–82. <https://doi.org/10.1148/radiol.14140244>.
- Mack MJ, Leon MB, Smith CR, et al. 5-year outcomes of transcatheter aortic valve replacement or surgical aortic valve replacement for high surgical risk patients with aortic stenosis (PARTNER 1): a randomised controlled trial. *Lancet* 2015;**385**(9986):2477–84. [https://doi.org/10.1016/S0140-6736\(15\)60308-7](https://doi.org/10.1016/S0140-6736(15)60308-7).
- Leon MB, Smith CR, Mack MJ, et al. Transcatheter or surgical aortic-valve replacement in intermediate-risk patients. *N Engl J Med* 2016;**374**(17):1609–20. <https://doi.org/10.1056/NEJMoa1514616>.
- Reardon MJ, Van Mieghem NM, Popma JJ, et al. Surgical or transcatheter aortic-valve replacement in intermediate-risk patients. *N Engl J Med* 2017;**376**(14):1321–31. <https://doi.org/10.1056/NEJMoa1700456>.
- Søndergaard L, Steinbrüchel DA, Ihlemann N, et al. Two-year outcomes in patients with severe aortic valve stenosis randomized to transcatheter versus surgical aortic valve replacement: the All-Comers Nordic Aortic Valve Intervention randomized clinical trial. *Circ Cardiovasc Interv* 2016;**9**(6):1–10. <https://doi.org/10.1161/CIRCINTERVENTIONS.115.003665>.
- Suchá D, Tuncay V, Prakken NHJ, et al. Does the aortic annulus undergo conformational change throughout the cardiac cycle? A systematic review. *Eur Heart J Cardiovasc Imag* 2015;**16**(12):1307–17. <https://doi.org/10.1093/ehjci/jev210>.

26. Jurecsek T, Turek J, Kietselaer BLJH, et al. MDCT evaluation of aortic root and aortic valve prior to TAVI. What is the optimal imaging time point in the cardiac cycle? *Eur Radiol* 2015;**25**(7):1975–83. <https://doi.org/10.1007/s00330-015-3607-5>.
27. Murphy DT, Blanke P, Alaamri S, et al. Dynamism of the aortic annulus: effect of diastolic versus systolic CT annular measurements on device selection in transcatheter aortic valve replacement (TAVR). *J Cardiovasc Comput Tomogr* 2016;**10**(1):37–43. <https://doi.org/10.1016/j.jcct.2015.07.008>.
28. Willson AB, Webb JG, Freeman M, et al. Computed tomography-based sizing recommendations for transcatheter aortic valve replacement with balloon-expandable valves: comparison with transesophageal echocardiography and rationale for implementation in a prospective trial. *J Cardiovasc Comput Tomogr* 2012;**6**(6):406–14. <https://doi.org/10.1016/j.jcct.2012.10.002>.
29. De Heer LM, Budde RPJ, Van Prehn J, et al. Pulsatile distention of the nondiseased and stenotic aortic valve annulus: analysis with electrocardiogram-gated computed tomography. *Ann Thorac Surg* 2012;**93**(2):516–22. <https://doi.org/10.1016/j.athoracsur.2011.08.068>.
30. Piazza N, de Jaegere P, Schultz C, et al. Anatomy of the aortic valvar complex and its implications for transcatheter implantation of the aortic valve. *Circ Cardiovasc Interv* 2008;**1**(1):74–81. <https://doi.org/10.1161/CIRCINTERVENTIONS.108.780858>.
31. Anderson RH. Clinical anatomy of the aortic root. *Heart* 2000;**84**(6):670–3. <https://doi.org/10.1136/heart.84.6.670>.
32. Masri A, Schoenhagen P, Svensson L, et al. Dynamic characterization of aortic annulus geometry and morphology with multimodality imaging: predictive value for aortic regurgitation after transcatheter aortic valve replacement. *J Thorac Cardiovasc Surg* 2014;**147**(6):1847–54. <https://doi.org/10.1016/j.jtcvs.2013.05.047>.
33. Elattar M, Wiegeler E, van Kesteren F, et al. Automatic aortic root landmark detection in CTA images for preprocedural planning of transcatheter aortic valve implantation. *Int J Cardiovasc Imag* 2016;**32**(3):501–11. <https://doi.org/10.1007/s10554-015-0793-9>.
34. Liang L, Kong F, Martin C, et al. Machine learning-based 3-D geometry reconstruction and modeling of aortic valve deformation using 3-D computed tomography images. *Int J Numer Method Biomed Eng* 2017;**33**(5):e2827. <https://doi.org/10.1002/cnm.2827>.
35. De Jaegere P, Rocatello G, Prendergast BD, et al. Patient-specific computer simulation for transcatheter cardiac interventions: what a clinician needs to know. *Heart* 2019;**105**:S21–7. <https://doi.org/10.1136/heartjnl-2018-313514>.
36. Schultz C, Rodriguez-Olivares R, Bosmans J, et al. Patient-specific image-based computer simulation for the prediction of valve morphology and calcium displacement after TAVI with the Medtronic CoreValve and the Edwards SAPIEN valve. *EuroIntervention* 2016;**11**(9):1044–52. <https://doi.org/10.4244/EIJV11I9A212>.
37. Bianchi M, Marom G, Ghosh RP, et al. Patient-specific simulation of transcatheter aortic valve replacement: impact of deployment options on paravalvular leakage. *Biomech Model Mechanobiol* 2019;**18**(2):435–51. <https://doi.org/10.1007/s10237-018-1094-8>.
38. De Jaegere P, De Santis G, Rodriguez-Olivares R, et al. Patient-specific computer modeling to predict aortic regurgitation after transcatheter aortic valve replacement. *JACC Cardiovasc Interv* 2016;**9**(5):508–12. <https://doi.org/10.1016/j.jcin.2016.01.003>.
39. Rocatello G, El Faquir N, De Santis G, et al. Patient-specific computer simulation to elucidate the role of contact pressure in the development of new conduction abnormalities after catheter-based implantation of a self-expanding aortic valve. *Circ Cardiovasc Interv* 2018;**11**(2):1–9. <https://doi.org/10.1161/CIRCINTERVENTIONS.117.005344>.
40. Mack MJ, Brennan JM, Brindis R, et al. Outcomes following transcatheter aortic valve replacement in the United States. *JAMA* 2013;**310**(19):2069–77. <https://doi.org/10.1001/jama.2013.282043>.
41. Mack MJ, Brennan JM, Brindis R, et al. Outcomes following transcatheter aortic valve replacement in the United States. *JAMA* 2013. <https://doi.org/10.1001/jama.2013.282043>.
42. Hayashida K, Bouvier E, Lefevre T, et al. Transcatheter aortic valve implantation for patients with severe bicuspid aortic valve stenosis. *Circ Cardiovasc Interv* 2013;**6**(3):284–91. <https://doi.org/10.1161/CIRCINTERVENTIONS.112.000084>.
43. Jilaihawi H, Chen M, Webb J, et al. A bicuspid aortic valve imaging classification for the TAVR era. *JACC Cardiovasc Imag* 2016;**9**(10):1145–58. <https://doi.org/10.1016/j.jcmg.2015.12.022>.
44. Amoretti F, Cerillo AG, Mariani M, et al. A simple method to visualize the bicuspid aortic valve pathology by cardiac computed tomography. *J Cardiovasc Comput Tomogr* 2019;(August):1–4. <https://doi.org/10.1016/j.jcct.2019.08.005> [in press].
45. Tchetché D, de Biase C, van Gils L, et al. Bicuspid aortic valve anatomy and relationship with devices: the BAVARD Multicenter Registry. *Circ Cardiovasc Interv* 2019;**12**(1):e007107. <https://doi.org/10.1161/CIRCINTERVENTIONS.118.007107>.
46. Hansson NC, Nørgaard BL, Barbanti M, et al. The impact of calcium volume and distribution in aortic root injury related to balloon-expandable transcatheter aortic valve replacement. *J Cardiovasc Comput Tomogr* 2015;**9**(5):382–92. <https://doi.org/10.1016/j.jcct.2015.04.002>.
47. Latsios G, Gerckens U, Buellesfeld L, et al. “Device landing zone” calcification, assessed by MSCT, as a predictive factor for pacemaker implantation after TAVI. *Cathet Cardiovasc Interv* 2010;**76**(3):431–9. <https://doi.org/10.1002/ccd.22563>.
48. Ewe SH, Ng ACT, Schuijff JD, et al. Location and severity of aortic valve calcium and implications for aortic regurgitation after transcatheter aortic valve implantation. *Am J Cardiol* 2011;**108**(10):1470–7. <https://doi.org/10.1016/j.amjcard.2011.07.007>.
49. Jilaihawi H, Makkar RR, Kashif M, et al. A revised methodology for aortic-valvar complex calcium quantification for transcatheter aortic valve implantation. *Eur Heart J Cardiovasc Imag* 2014;**15**(12):1324–32. <https://doi.org/10.1093/ehjci/jeu162>.
50. Khalique OK, Hahn RT, Gada H, et al. Quantity and location of aortic valve complex calcification predicts severity and location of paravalvular regurgitation and frequency of post-dilation after balloon-expandable transcatheter aortic valve replacement. *JACC Cardiovasc Interv* 2014;**7**(8):885–94. <https://doi.org/10.1016/j.jcin.2014.03.007>.
51. Abramowitz Y, Jilaihawi H, Chakravarty T, et al. Balloon-expandable transcatheter aortic valve replacement in patients with extreme aortic valve calcification. *Cathet Cardiovasc Interv* 2016;**87**(6):1173–9. <https://doi.org/10.1002/ccd.26311>.
52. Hansson NC, Leipsic J, Pugliese F, et al. Aortic valve and left ventricular outflow tract calcium volume and distribution in transcatheter aortic valve replacement: influence on the risk of significant paravalvular regurgitation. *J Cardiovasc Comput Tomogr* 2018;**12**(4):290–7. <https://doi.org/10.1016/j.jcct.2018.02.002>. September 2017.
53. Tzikas A, Schultz C, Van Mieghem NM, et al. Optimal projection estimation for transcatheter aortic valve implantation based on contrast-aortography: validation of a prototype software. *Cathet Cardiovasc Interv* 2010;**76**(4):602–7. <https://doi.org/10.1002/ccd.22641>.
54. Arnold M, Achenbach S, Pfeiffer I, et al. A method to determine suitable fluoroscopic projections for transcatheter aortic valve implantation by computed tomography. *J Cardiovasc Comput Tomogr* 2012;**6**(6):422–8. <https://doi.org/10.1016/j.jcct.2012.10.008>.
55. Binder RK, Leipsic J, Wood D, et al. Prediction of optimal deployment projection for transcatheter aortic valve replacement: angiographic 3-dimensional reconstruction of the aortic root versus multidetector computed tomography. *Circ Cardiovasc Interv* 2012;**5**(2):247–52. <https://doi.org/10.1161/CIRCINTERVENTIONS.111.966531>.
56. Cockburn J, Trivedi U, Belder A De, et al. Optimal projection for transcatheter aortic valve implantation determined from the reference projection angles. *Cathet Cardiovasc Interv* 2012;**80**(6):973–7. <https://doi.org/10.1002/ccd.23393>.
57. Dvir D, Kornowski R. Percutaneous aortic valve implantation using novel imaging guidance. *Cathet Cardiovasc Interv* 2010;**76**(3):450–4. <https://doi.org/10.1002/ccd.22362>.
58. Gurvitch R, Wood DA, Leipsic J, et al. Multislice computed tomography for prediction of optimal angiographic deployment projections during transcatheter aortic valve implantation. *JACC Cardiovasc Interv* 2010;**3**(11):1157–65. <https://doi.org/10.1016/j.jcin.2010.09.010>.
59. Kurra V, Kapadia SR, Tuzcu EM, et al. Pre-procedural imaging of aortic root orientation and dimensions. comparison between X-ray angiographic planar imaging and 3-dimensional multidetector row computed tomography. *JACC Cardiovasc Interv* 2010;**3**(1):105–13. <https://doi.org/10.1016/j.jcin.2009.10.014>.

60. Samim M, Stella PR, Agostoni P, et al. Automated 3D analysis of pre-procedural MDCT to predict annulus plane angulation and C-arm positioning: benefit on procedural outcome in patients referred for TAVR. *JACC Cardiovasc Imag* 2013;**6**(2):238–48. <https://doi.org/10.1016/j.jcmg.2012.12.004>.
61. Kempfert J, Falk V, Schuler G, et al. Dyna-CT during minimally invasive off-pump transapical aortic valve implantation. *Ann Thorac Surg* 2009;**88**(6):2041. <https://doi.org/10.1016/j.athoracsur.2009.01.029>.
62. Poon KK, Crowhurst J, James C, et al. Impact of optimising fluoroscopic implant angles on paravalvular regurgitation in transcatheter aortic valve replacements — utility of three-dimensional rotational angiography. *EuroIntervention* 2012;**8**(5):538–45. <https://doi.org/10.4244/EIJV8I5A84>.
63. Hell MM, Biburger L, Marwan M, et al. Prediction of fluoroscopic angulations for transcatheter aortic valve implantation by CT angiography: influence on procedural parameters. *Eur Heart J Cardiovasc Imag* 2017;**18**(8):906–14. <https://doi.org/10.1093/ehjci/jew144>.
64. Kim W-K, Renker M, Rolf A, et al. Annular versus supra-annular sizing for TAVI in bicuspid aortic valve stenosis. *EuroIntervention* 2019;**15**(3):e231–8. <https://doi.org/10.4244/eij-d-19-00236>.
65. Barbanti M, Buccheri S, Rodès-Cabau J, et al. Transcatheter aortic valve replacement with new-generation devices: a systematic review and meta-analysis. *Int J Cardiol* 2017;**245**:83–9. <https://doi.org/10.1016/j.ijcard.2017.07.083>.
66. Barbanti M, Yang TH, Rodès Cabau J, et al. Anatomical and procedural features associated with aortic root rupture during balloon-expandable transcatheter aortic valve replacement. *Circulation* 2013;**128**(3):244–53. <https://doi.org/10.1161/CIRCULATIONAHA.113.02947>.
67. Ribeiro HB, Webb JG, Makkar RR, et al. Predictive factors, management, and clinical outcomes of coronary obstruction following transcatheter aortic valve implantation: insights from a large multicenter registry. *J Am Coll Cardiol* 2013;**62**(17):1552–62. <https://doi.org/10.1016/j.jacc.2013.07.040>.
68. Ribeiro HB, Nombela-Franco L, Urena M, et al. Coronary obstruction following transcatheter aortic valve implantation: a systematic review. *JACC Cardiovasc Interv* 2013;**6**(5):452–61. <https://doi.org/10.1016/j.jcin.2012.11.014>.
69. Kodali S, Pibarot P, Douglas PS, et al. Paravalvular regurgitation after transcatheter aortic valve replacement with the Edwards Sapien valve in the PARTNER trial: characterizing patients and impact on outcomes. *Eur Heart J* 2015;**36**(7):449–56. <https://doi.org/10.1093/eurheartj/ehu384>.
70. Pibarot P, Hahn RT, Weissman NJ, et al. Association of paravalvular regurgitation with 1-year outcomes after transcatheter aortic valve replacement with the SAPIEN 3 valve. *JAMA Cardiol* 2017;**2**(11):1208. <https://doi.org/10.1001/jamacardio.2017.3425>.
71. Vasa-Nicotera M, Sinning JM, Chin D, et al. Impact of paravalvular leakage on outcome in patients after transcatheter aortic valve implantation. *JACC Cardiovasc Interv* 2012;**5**(8):858–65. <https://doi.org/10.1016/j.jcin.2012.04.011>.
72. Jilaihawi H, Kashif M, Fontana G, et al. Cross-sectional computed tomographic assessment improves accuracy of aortic annular sizing for transcatheter aortic valve replacement and reduces the incidence of paravalvular aortic regurgitation. *J Am Coll Cardiol* 2012;**59**(14):1275–86. <https://doi.org/10.1016/j.jacc.2011.11.045>.
73. Sherif MA, Abdel-Wahab M, Stöcker B, et al. Anatomic and procedural predictors of paravalvular aortic regurgitation after implantation of the medtronic CoreValve bioprosthesis. *J Am Coll Cardiol* 2010;**56**(20):1623–9. <https://doi.org/10.1016/j.jacc.2010.06.035>.
74. Yousef A, Simard T, Webb J, et al. Transcatheter aortic valve implantation in patients with bicuspid aortic valve: a patient level multi-center analysis. *Int J Cardiol* 2015;**189**(1):282–8. <https://doi.org/10.1016/j.ijcard.2015.04.066>.
75. Yoon S-H, Bleiziffer S, De Backer O, et al. Outcomes in transcatheter aortic valve replacement for bicuspid versus tricuspid aortic valve stenosis. *J Am Coll Cardiol* 2017;**69**(21):2579–89. <https://doi.org/10.1016/j.jacc.2017.03.017>.
76. Kochman J, Huczek Z, Ścisło P, et al. Comparison of one- and 12-month outcomes of transcatheter aortic valve replacement in patients with severely stenotic bicuspid versus tricuspid aortic valves (results from a multicenter registry). *Am J Cardiol* 2014;**114**(5):757–62. <https://doi.org/10.1016/j.amjcard.2014.05.063>.
77. Sannino A, Cedars A, Stoler RC, et al. Comparison of efficacy and safety of transcatheter aortic valve implantation in patients with bicuspid vs tricuspid aortic valves. *Am J Cardiol* 2017;**120**(9):1601–6. <https://doi.org/10.1016/j.amjcard.2017.07.053>.
78. Hamdan A, Guetta V, Klempfner R, et al. Inverse relationship between membranous septal length and the risk of atrioventricular block in patients undergoing transcatheter aortic valve implantation. *JACC Cardiovasc Interv* 2015;**8**(9):1218–28. <https://doi.org/10.1016/j.jcin.2015.05.010>.
79. Ruile P, Pache G, Minners J, et al. Fusion imaging of pre- and post-procedural computed tomography angiography in transcatheter aortic valve implantation patients: evaluation of prosthesis position and its influence on new conduction disturbances. *Eur Hear J Cardiovasc Imag* 2019;**20**(7):781–8. <https://doi.org/10.1093/ehjci/jev195>.
80. Maeno Y, Abramowitz Y, Kawamori H, et al. A highly predictive risk model for pacemaker implantation after TAVR. *JACC Cardiovasc Imag* 2017;**10**(10):1139–47. <https://doi.org/10.1016/j.jcmg.2016.11.020>.
81. Fujita B, Kütting M, Seiffert M, et al. Calcium distribution patterns of the aortic valve as a risk factor for the need of permanent pacemaker implantation after transcatheter aortic valve implantation. *Eur Hear J Cardiovasc Imag* 2016;**17**(12):1385–93. <https://doi.org/10.1093/ehjci/jev343>.
82. Jilaihawi H, Zhao Z, Du R, et al. Minimizing permanent pacemaker following repositionable self-expanding transcatheter aortic valve replacement. *JACC Cardiovasc Interv* 2019;**12**(18):1796–807. <https://doi.org/10.1016/j.jcin.2019.05.056>.
83. Tchétché D, Windecker S, Kasel AM, et al. 1-Year outcomes of the CENTERA-EU trial assessing a novel self-expanding transcatheter heart valve. *JACC Cardiovasc Interv* 2019;**12**(7):673–80. <https://doi.org/10.1016/j.jcin.2019.01.231>.
84. Baumgartner H, Falk V, Bax JJ, et al. ESDG. 2017 ESC/EACTS guidelines for the management of valvular heart disease. *Eur Heart J* 2017;**38**:2739–91. <https://doi.org/10.1093/eurheartj/ehx391.2017>.
85. Nishimura RA, Otto CM. 2017 AHA/ACC focused update of the 2014 AHA/ACC guideline for the management of patients with valvular heart disease: a report of the American College of Cardiology/American Heart Association Task Force on Clinical Practice Guidelines. *Circulation* June 20, 2017;**135**(25):e1161–95. <https://doi.org/10.1161/CIR.0000000000000503>.
86. Overtchouk P, Modine T. Alternate access for TAVI: stay clear of the chest. *Interv Cardiol Rev* 2018;**13**(3):145–50. <https://doi.org/10.15420/icr.2018.22.1>.
87. Van Mieghem NM, Tchetché D, Chieffo A, et al. Incidence, predictors, and implications of access site complications with transfemoral transcatheter aortic valve implantation. *Am J Cardiol* 2012;**110**(9):1361–7. <https://doi.org/10.1016/j.amjcard.2012.06.042>.
88. Tamburino C, Capodanno D, Ramondo A, et al. Incidence and predictors of early and late mortality after transcatheter aortic valve implantation in 663 patients with severe aortic stenosis. *Circulation* 2011;**123**(3):299–308. <https://doi.org/10.1161/CIRCULATIONAHA.110.946533>.
89. Okuyama K, Jilaihawi H, Kashif M, et al. Transfemoral access assessment for transcatheter aortic valve replacement: evidence-based application of computed tomography over invasive angiography. *Circ Cardiovasc Imag* 2014;**8**(1). <https://doi.org/10.1161/CIRCIMAGING.114.001995>.
90. Auffret V, Lefevre T, Van Belle E, et al. Temporal trends in transcatheter aortic valve replacement in France: France 2 to France TAVI. *J Am Coll Cardiol* 2017. <https://doi.org/10.1016/j.jacc.2017.04.053>.
91. Wee IJY, Stonier T, Harrison M, et al. Transcatheter aortic valve implantation: a systematic review. *J Cardiol* 2018;**71**(6):525–33. <https://doi.org/10.1016/j.jicc.2018.01.010>.
92. Gleason TG, Schindler JT, Hagberg RC, et al. Subclavian/axillary access for self-expanding transcatheter aortic valve replacement renders equivalent outcomes as transfemoral. *Ann Thorac Surg* 2018;**105**(2):477–83. <https://doi.org/10.1016/j.athoracsur.2017.07.017>.
93. Greenbaum AB, Babaliaros VC, Chen MY, et al. Transcaval access and closure for transcatheter aortic valve replacement: a prospective

- investigation. *J Am Coll Cardiol* 2017;**69**(5):511–21. <https://doi.org/10.1016/j.jacc.2016.10.024>.
94. Søndergaard L, Popma JJ, Reardon MJ, et al. Comparison of a complete percutaneous versus surgical approach to aortic valve replacement and revascularization in patients at intermediate surgical risk: results from the randomized SURTAVI trial. *Circulation* 2019;**140**:1296–305. <https://doi.org/10.1161/circulationaha.118.039564>.
  95. Rossi A, De Cecco CN, Kennon SRO, et al. CT angiography to evaluate coronary artery disease and revascularization requirement before transcatheter aortic valve replacement. *J Cardiovasc Comput Tomogr* 2017;**11**(5):338–46. <https://doi.org/10.1016/j.jcct.2017.06.001>.
  96. Chaikriangkrai K, Jhun HY, Shantha GPS, et al. Diagnostic accuracy of coronary computed tomography before aortic valve replacement: systematic review and meta-analysis. *J Thorac Imag* 2018;**33**(4):207–16. <https://doi.org/10.1097/RTI.0000000000000322>.
  97. Kotronias RA, Kwok CS, George S, et al. Transcatheter aortic valve implantation with or without percutaneous coronary artery revascularization strategy: a systematic review and meta-analysis. *J Am Heart Assoc* 2017;**6**(6):e005960. <https://doi.org/10.1161/JAHA.117.005960>.
  98. Yang Y, Huang F, Huang B, et al. The safety of concomitant transcatheter aortic valve replacement and percutaneous coronary intervention. *Med* 2017;**96**(48):1–6. <https://doi.org/10.1097/MD.00000000000008919>.
  99. van Kesteren F, Wiegerinck EMA, van Mourik MS, et al. Impact of potentially malignant incidental findings by computed tomographic angiography on long-term survival after transcatheter aortic valve implantation. *Am J Cardiol* 2017;**120**(6):994–1001. <https://doi.org/10.1016/j.amjcard.2017.06.032>.
  100. Stachon P, Kaier K, Milde S, et al. Two-year survival of patients screened for transcatheter aortic valve replacement with potentially malignant incidental findings in initial body computed tomography. *Eur Heart J Cardiovasc Imag* 2015;**16**(7):731–7. <https://doi.org/10.1093/ehjci/jev055>.
  101. Lindsay AC, Sriharan M, Lazoura O, et al. Clinical and economic consequences of non-cardiac incidental findings detected on cardiovascular computed tomography performed prior to transcatheter aortic valve implantation (TAVI). *Int J Cardiovasc Imag* 2015;**31**(7):1435–46. <https://doi.org/10.1007/s10554-015-0685-z>.
  102. Leon MB, Piazza N, Nikolsky E, et al. Standardized endpoint definitions for transcatheter aortic valve implantation clinical trials: a consensus report from the Valve Academic Research Consortium. *Eur Heart J* 2011;**32**(2):205–17. <https://doi.org/10.1093/eurheartj/ehq406>.
  103. Kappetein AP, Head SJ, Généreux P, et al. Updated standardized endpoint definitions for transcatheter aortic valve implantation. *J Am Coll Cardiol* 2012;**60**(15):1438–54. <https://doi.org/10.1016/j.jacc.2012.09.001>.
  104. Salgado RA, Budde RPJ, Leiner T, et al. Transcatheter aortic valve replacement: postoperative CT findings of Sapien and CoreValve transcatheter heart valves. *RadioGraphics* 2014;**34**(6):1517–36. <https://doi.org/10.1148/rg.346130149>.
  105. Blanke P, Schoepf UJ, Leipsic JA. CT in transcatheter aortic valve replacement. *Radiology* 2013;**269**(3):650–69. <https://doi.org/10.1148/radiol.13120696>.
  106. Symersky P, Budde RPJ, Prokop M, et al. Multidetector-row computed tomography imaging characteristics of mechanical prosthetic valves. *J Heart Valve Dis* 2011;**20**(2):216–22.
  107. Willson AB, Webb JG, Labounty TM, et al. 3-dimensional aortic annular assessment by multidetector computed tomography predicts moderate or severe paravalvular regurgitation after transcatheter aortic valve replacement: a multicenter retrospective analysis. *J Am Coll Cardiol* 2012;**59**(14):1287–94. <https://doi.org/10.1016/j.jacc.2011.12.015>.
  108. Willson AB, Webb JG, Gurvitch R, et al. Structural integrity of balloon-expandable stents after transcatheter aortic valve replacement: assessment by multidetector computed tomography. *JACC Cardiovasc Interv* 2012;**5**(5):525–32. <https://doi.org/10.1016/j.jcin.2012.03.007>.
  109. Binder RK, Webb JG, Toggweiler S, et al. Impact of post-implant SAPIEN XT geometry and position on conduction disturbances, hemodynamic performance, and paravalvular regurgitation. *JACC Cardiovasc Interv* 2013;**6**(5):462–8. <https://doi.org/10.1016/j.jcin.2012.12.128>.
  110. Tan JS, Leipsic J, Perlman G, et al. A strategy of underexpansion and ad hoc post-dilation of balloon-expandable transcatheter aortic valves in patients at risk of annular injury favorable mid-term outcomes. *JACC Cardiovasc Interv* 2015;**8**(13):1727–32. <https://doi.org/10.1016/j.jcin.2015.08.011>.
  111. Gooley RP, Cameron JD, Meredith IT. Assessment of the geometric interaction between the lotus transcatheter aortic valve prosthesis and the native ventricular aortic interface by 320-multidetector computed tomography. *JACC Cardiovasc Interv* 2015;**8**(5):740–9. <https://doi.org/10.1016/j.jcin.2015.03.002>.
  112. Bekeredjian R, Bodingbauer D, Hofmann NP, et al. The extent of aortic annulus calcification is a predictor of postprocedural eccentricity and paravalvular regurgitation: a pre- and postinterventional cardiac computed tomography angiography study. *J Invasive Cardiol* 2015;**27**(3):172–80.
  113. Schuhbaeck A, Weingartner C, Arnold M, et al. Aortic annulus eccentricity before and after transcatheter aortic valve implantation: comparison of balloon-expandable and self-expanding prostheses. *Eur J Radiol* 2015;**84**(7):1242–8. <https://doi.org/10.1016/j.ejrad.2015.04.003>.
  114. Leetmaa T, Hansson NC, Leipsic J, et al. Early aortic transcatheter heart valve thrombosis: diagnostic value of contrast-enhanced multidetector computed tomography. *Circ Cardiovasc Interv* 2015;**8**(4):1–9. <https://doi.org/10.1161/CIRCINTERVENTIONS.114.001596>.
  115. Pache G, Schoeclin S, Blanke P, et al. Early hypo-attenuated leaflet thickening in balloon-expandable transcatheter aortic heart valves. *Eur Heart J* 2016;**37**(28):2263–71. <https://doi.org/10.1093/eurheartj/ehv526>.
  116. Makkar RR, Fontana G, Jiliahawi H, et al. Possible subclinical leaflet thrombosis in bioprosthetic aortic valves. *N Engl J Med* 2015;**373**(21):2015–24. <https://doi.org/10.1056/NEJMoa1509233>.
  117. Hansson NC, Grove EL, Andersen HR, et al. Transcatheter aortic valve thrombosis: incidence, predisposing factors, and clinical implications. *J Am Coll Cardiol* 2016;**68**(19):2059–69. <https://doi.org/10.1016/j.jacc.2016.08.010>.
  118. Yanagisawa R, Hayashida K, Yamada Y, et al. Incidence, predictors, and mid-term outcomes of possible leaflet thrombosis after TAVR. *JACC Cardiovasc Imag* 2017;**10**(1):1–11. <https://doi.org/10.1016/j.jcmg.2016.11.005>.
  119. Gündüz S, Özkan M, Kalçık M, et al. Sixty-four-section cardiac computed tomography in mechanical prosthetic heart valve dysfunction: thrombus or pannus. *Circ Cardiovasc Imag* 2015;**8**(12):1–11. <https://doi.org/10.1161/CIRCIMAGING.115.003246>.
  120. Søndergaard L, De Backer O, Kofoed KF, et al. Natural history of sub-clinical leaflet thrombosis affecting motion in bioprosthetic aortic valves. *Eur Heart J* 2017, <https://doi.org/10.1093/eurheartj/ehx369> (January):2201–7.
  121. Landes U, Kornowski R. Transcatheter valve implantation in degenerated bioprosthetic surgical valves (ViV) in aortic, mitral, and tricuspid positions: a review. *Struct Heart* 2017;**1**(5–6):225–35. <https://doi.org/10.1080/24748706.2017.1372649>. 00(00).
  122. Webb JG, Murdoch DJ, Alu MC, et al. 3-Year outcomes after valve-in-valve transcatheter aortic valve replacement for degenerated bioprostheses: the PARTNER 2 Registry. *J Am Coll Cardiol* 2019;**73**(21):2647–55. <https://doi.org/10.1016/j.jacc.2019.03.483>.
  123. Ribeiro HB, Rodés-Cabau J, Blanke P, et al. Incidence, predictors, and clinical outcomes of coronary obstruction following transcatheter aortic valve replacement for degenerative bioprosthetic surgical valves: insights from the VIVID registry. *Eur Heart J* 2018;**39**(8):687–95. <https://doi.org/10.1093/eurheartj/ehx455>.
  124. Blanke P, Soon J, Dvir D, et al. Computed tomography assessment for transcatheter aortic valve in valve implantation: the Vancouver approach to predict anatomical risk for coronary obstruction and other considerations. *J Cardiovasc Comput Tomogr* 2016;**10**(6):491–9. <https://doi.org/10.1016/j.jcct.2016.09.004>.
  125. Suchá D, Daans CG, Symersky P, et al. Reliability, agreement, and presentation of a reference standard for assessing implanted heart valve sizes by multidetector-row computed tomography. *Am J Cardiol* 2015;**116**(1):112–20. <https://doi.org/10.1016/j.amjcard.2015.03.048>.
  126. Bapat VN, Attia R, Thomas M. Effect of valve design on the stent internal diameter of a bioprosthetic valve: a concept of true internal diameter and its implications for the valve-in-valve procedure. *JACC Cardiovasc Interv* 2014;**7**(2):115–27. <https://doi.org/10.1016/j.jcin.2013.10.012>.

127. Costa G, Criscione E, Todaro D, et al. Long-term transcatheter aortic valve durability. *Interv Cardiol Rev* 2019;**14**(2):62. <https://doi.org/10.15420/icr.2019.4.2>.
128. Barbanti M, Webb JG, Tamburino C, et al. Outcomes of redo transcatheter aortic valve replacement for the treatment of postprocedural and late occurrence of paravalvular regurgitation and transcatheter valve failure. *Circ Cardiovasc Interv* 2016;**9**(9):1–10. <https://doi.org/10.1161/CIRCINTERVENTIONS.116.003930>.
129. Blumenstein J, Kim WK, Liebetrau C, et al. Challenges of coronary angiography and intervention in patients previously treated by TAVI. *Clin Res Cardiol* 2015;**104**(8):632–9. <https://doi.org/10.1007/s00392-015-0824-5>.
130. Yudi MB, Sharma SK, Tang GHL, et al. Coronary angiography and percutaneous coronary intervention after transcatheter aortic valve replacement. *J Am Coll Cardiol* 2018;**71**(12):1360–78. <https://doi.org/10.1016/j.jacc.2018.01.057>.
131. Jabbour RJ, Tanaka A, Finkelstein A, et al. Delayed coronary obstruction after transcatheter aortic valve replacement. *J Am Coll Cardiol* 2018;**71**(14):1513–24. <https://doi.org/10.1016/j.jacc.2018.01.066>.
132. Katsanos S, Debonnaire P, Van Der Kley F, et al. Position of Edwards SAPIEN transcatheter valve in the aortic root in relation with the coronary ostia: implications for percutaneous coronary interventions. *Cathet Cardiovasc Interv* 2015;**85**(3):480–7. <https://doi.org/10.1002/ccd.25718>.